Received: 21 November 2018 | Revised: 27 April 2020 | Accepted: 27 April 2020

DOI: 10.1002/cne.24938

RESEARCH ARTICLE

JCN RESEARCH IN SYSTEMS NEUROSCIENCE THE JOURNAL OF COMPARATIVE NEUROLOGY WILEY

Serotonin distribution in the brain of the plainfin midshipman: Substrates for vocal-acoustic modulation and a reevaluation of the serotonergic system in teleost fishes

Miky Timothy[1] | Paul M. Forlano[1,2,3,4,5]

[1]Department of Biology, Brooklyn College, City University of New York, 2900 Bedford Avenue, Brooklyn, New York, 11210

[2]Biology Subprogram in Ecology, Evolution, and Behavior, The Graduate Center, City University of New York, 365 5th Avenue, New York, New York, 10016

[3]Biology Subprogram in Neuroscience, The Graduate Center, City University of New York, 365 5th Avenue, New York, New York, 10016

[4]Psychology Subprogram in Behavioral and Cognitive Neuroscience, The Graduate Center, City University of New York, 365 5th Avenue, New York, New York, 10016

[5]Aquatic Research and Environmental Assessment Center, Brooklyn College, Brooklyn, New York

Correspondence
Miky Timothy, Paul M. Forlano, Department of Biology, Brooklyn College, City University of New York, 2900 Bedford Avenue, Brooklyn, NY, 11210, USA.
Email: mikytimothy@gmail.com; pforlano@brooklyn.cuny.edu

Abstract

Serotonin (5-HT) is a modulator of neural circuitry underlying motor patterning, homeostatic control, and social behavior. While previous studies have described 5-HT distribution in various teleosts, serotonergic raphe subgroups in fish are not well defined and therefore remain problematic for cross-species comparisons. Here we used the plainfin midshipman fish, *Porichthys notatus*, a well-studied model for investigating the neural and hormonal mechanisms of vertebrate vocal-acoustic communication, to redefine raphe subgroups based on both stringent neuroanatomical landmarks as well as quantitative cell measurements. In addition, we comprehensively characterized 5-HT-immunoreactive (-ir) innervation throughout the brain, including well-delineated vocal and auditory nuclei. We report neuroanatomical heterogeneity in populations of the serotonergic raphe nuclei of the brainstem reticular formation, with three discrete subregions in the superior raphe, an intermediate 5-HT-ir cell cluster, and an extensive inferior raphe population. 5-HT-ir neurons were also observed within the vocal motor nucleus (VMN), forming putative contacts on those cells. In addition, three major 5-HT-ir cell groups were identified in the hypothalamus and one group in the pretectum. Significant 5-HT-ir innervation was found in components of the vocal pattern generator and cranial motor nuclei. All vocal midbrain nuclei showed considerable 5-HT-ir innervation, as did thalamic and hindbrain auditory and lateral line areas and vocal-acoustic integration sites in the preoptic area and ventral telencephalon. This comprehensive atlas offers new insights into the organization of 5-HT nuclei in teleosts and provides neuroanatomical evidence for serotonin as a modulator of vocal-acoustic circuitry and behavior in midshipman fish, consistent with findings in vocal tetrapods.

KEYWORDS

5-HT, auditory, cranial motor, raphe, teleost, vocal pattern generator

1 | INTRODUCTION

Serotonin, or 5-hydroxytryptamine (5-HT), is a monoamine neurotransmitter found in all vertebrates that regulates an exceptional diversity of physiological and behavioral activity. The variety of biological functions in which serotonin plays a part can be partly explained through its variety of receptor profiles—up to seven families with at least 15 subtypes in humans (Berger, Gray, & Roth, 2009). It has also been proposed that the complexity of serotonergic neuronal modulation may originate in the anatomical segregation of separately

and at times exclusively projecting nuclei coupled with unique neurochemical profiles (Gaspar & Lillesaar, 2012; Kiyasova et al, 2011; Pollak Dorocic et al., 2014; Vertes & Linley, 2008).

The 5-HT system is perhaps best known for the variety of pharmacological applications (also modeled in fish) that target the system in treatments in the areas of psychiatry, neurology, and metabolic science (Maximino & Herculano, 2010; Mennigen, Stroud, Zamora, Moon, & Trudeau, 2011), as well as being the primary target for classical hallucinogens, and likewise shown to have activity in fish (Hanks & González-Maeso, 2013; Neelkantan et al., 2013). Its role in coordinating fish swimming behavior has been well documented (Gabriel et al., 2009) with substantial research also performed on 5-HT regulation of teleostean hormonal regulation, social behavior, and aggression (Backström & Winberg, 2017; Dahlbom et al, 2012).

The neuroanatomical distribution of serotonin, notably in the brainstem raphe, is highly conserved across taxa, including teleost fishes (Lillesaar, 2011). The relative location of the serotonergic raphe nuclei appears to be a predictable feature in teleosts, and the teleostean raphe is generally believed to be anatomically homologous to the mammalian raphe (Lillesaar, Tannhäuser, Stigloher, Kremmer, & Bally-Cuif, 2007). While the roles in higher order behavior and cognition of the most rostral populations of brain stem serotonin cells (especially the dorsal and median raphe nuclei) have received substantial attention, the behavioral implications of the medullar serotonergic nuclei are not well understood. Evidence indicates that serotonergic tone is autoregulatory (Andrade, Huereca, Lyons, Andrade, & McGregor, 2015) and works through numerous downstream neurotransmitter intermediates (Fink & Göthert, 2007) thus making difficult the elucidation of its direct and naturalistic functional connections. Therefore, it is important to the understanding of its role in higher order and contextually relevant behaviors that 5-HT is studied in ethologically-based behavioral model organisms and the anatomical description of the 5-HT system in these species is crucial for this task. In zebra finches, serotonin, via 5-HT2 receptors, increases excitability in telencephalic neurons necessary for song production (Wood, Lovell, Mello, & Perkel, 2011). 5-HT has been shown to directly modulate the vocal physiology of mating calls of African clawed frogs (*Xenopus laevis*) and has been localized in the vocal pattern generator (VPG) in this species (Rhodes, Yu, & Yamaguchi, 2007; Yu & Yamaguchi, 2009; Yu & Yamaguchi, 2010). In gymnotiform fishes, 5-HT fibers are found in thalamic nuclei controlling electrocommunicative "chirps" (Telgkamp, Combs, & Smith, 2007) and 5-HT has shown to selectively modulate electroreceptive perception of conspecific electrical signals (Deemyad, Metzen, Pan, & Chacron, 2013).

The plainfin midshipman, *P. notatus*, presents two perspectives as a model in a mapping study of CNS serotonin. First, the significance of vocal and auditory-driven behaviors in midshipman reproductive tactics has resulted in a wealth of data regarding the neural circuitry involved in those behaviors (Forlano & Bass, 2011; Forlano, Sisneros, Rohmann, & Bass, 2015); Feng & Bass, 2017). Second, the presence of two male morphs utilizing different reproductive strategies presents an opportunity to study the endocrine, anatomical, and physiological basis of intraspecies social dynamics (Bass, 2008; Feng & Bass, 2017). Type I males build and defend nests and then court females using an advertisement call. Type II males are much smaller and do not vocalize as a reproductive tactic. Instead, they sneak spawn to steal egg fertilizations. Females exhibit a phonotaxic response to Type I calls and spawn once they have located the nest (Bass, 1996; Bass & McKibben, 2003; Bass et al., 1996). While only Type I males can produce a long duration advertisement call, all three adult reproductive morphs can produce isolated agonistic grunts (Bass & McKibben, 2003; McIver, Marchaterre, Rice, & Bass, 2014).

The neuroanatomical circuitry underlying vocalization in midshipman and other toadfish is well characterized (see Figure 1a). Descending nodes responsible for vocal initiation are found in the preoptic area and the anterior hypothalamus, send descending connections to midbrain vocal nuclei in the periaqueductal gray (PAG), paratoral, and isthmal nucleus, and project to the hindbrain VPG, which sets the temporal pattern of nerve impulses that terminate on sound-generating vocal muscles on the swim bladder (Figure 1a; Bass et al., 1994; Chagnaud, Baker, & Bass, 2011; Goodson & Bass, 2002; Kittelberger & Bass, 2012; Kittelberger et al., 2006; Feng & Bass, 2017). The VPG consists of paired lateral columns of three serially connected descending nodes: a vocal prepacemaker (VPP) nucleus that receives input from the midbrain and sets call duration, a vocal pacemaker nucleus involved in firing frequency, and a VMN dictating amplitude (Bass, Chagnaud, & Feng, 2015). Vocal circuitry shows interconnectivity with thalamic and medullar auditory nuclei as well as higher order telencephalic regions (Goodson & Bass, 2002). A recent study in the vocal Gulf toadfish (*Opsanus beta*) described 5-HT-ir in the hindbrain VPG of that related species (Rosner, Rohmann, Bass, & Chagnaud, 2018). This study investigates the distribution and morphology of the serotonin system in the entire brain of the plainfin midshpman and with a focus on evolutionarily conserved vocal and auditory circuitry.

The functional neuroanatomy of midshipman auditory circuitry has likewise been described. The saccule is the main auditory end organ and contains hair cells that synapse on primary afferents projecting to first-order medullary neurons comprising the descending octaval nucleus and its subdivisions and secondary octaval nuclei. These send afferents to the midbrain torus semicircularis, which in turn projects to several diencephalic nuclei including the anterior tuberal hypothalamus and central posterior thalamus, which relay information to telencephalic nuclei (Figure 1a; Forlano, Maruska, Sisneros, & Bass, 2016).

The goal of this study was to use immunohistochemistry (IHC) to (a) Characterize 5-HT-ir fiber projections throughout the entire brain of *P. notatus*, with emphasis on the innervation of identified auditory and vocal circuitry, (b) Define serotonergic nuclei into anatomical and morphological subgroups. Furthermore, we performed morphometric analyses (cell counts and cross-sectional area measures) to quantitatively define distinct subregions of the midshipman serotonergic raphe. Results herein provide a well-delineated neuroanatomical framework for comparative studies on the serotonergic system across fishes and other vertebrates. In addition, we provide strong evidence that serotonin acts as a modulator of both vocal and auditory circuitry

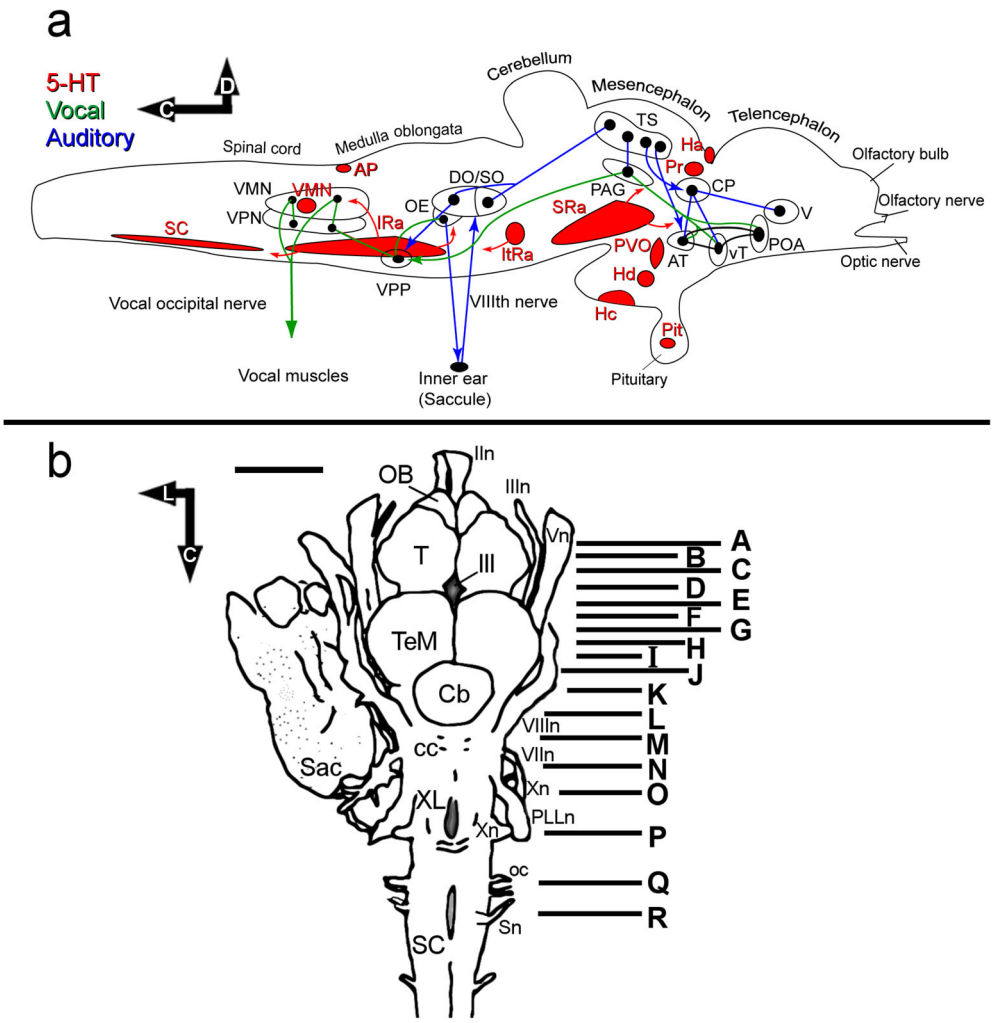

FIGURE 1 (a) Schematic sagittal view of the brain showing vocal motor (green) and central auditory (blue) systems in batrachoidid fish—plainfin midshipman and toadfish (modified from Bass & McKibben, 2003; Kittelberger, Land, & Bass, 2006). Black, bidirectional arrow indicates caudal (C) and dorsal (D) directions. Solid dots represent somata, and lines represent axonal projection pathways. Two connected dots indicate reciprocal connections. *Descending vocal motor pathways* (Bass & Baker, 1990; Bass, Marchaterre, & Baker, 1994; Bass et al., 2000; Bass et al., 2001; Fine & Perini, 1994; Goodson & Bass, 2002; Kittelberger et al., 2006; Remage-Healey & Bass, 2004): Preoptic (POA) and ventral (VT) and anterior (AT) tuberal nuclei in the hypothalamic forebrain project to the periaqueductal gray (PAG) in the midbrain, which then connects to the vocal pattern generator (VPG) in the hindbrain–spinal cord. The VPG consists of vocal prepacemaker (VPP), pacemaker (VPN), and motor (VMN) nuclei. The VMN projects directly via occipital nerve roots to sound-producing muscle on the swim bladder. *Central auditory system* (Bass et al., 1994; Bass et al., 2000; Bass et al., 2001): Social vocalizations are detected by the inner ear, which projects via the VIIIth nerve to descending (DO) and secondary (SO) octaval nuclei in the hindbrain and further to the auditory midbrain torus semicircularis (TS). Shown are nuclei interconnected with the TS. The dorsal thalamic central posterior nucleus (CP) contains reciprocal connections with the ventral telencephalon (V; includes the supracommissural division Vs) and anterior hypothalamus (AT/VT). The TS and CP also connect to vocal motor nuclei in the forebrain (AT, VT, and POA) and midbrain (PAG; isthmal/tegmentum [not shown]), whereas auditory-recipient octaval nuclei in the hindbrain connect to the VPG via the VPP (Bass et al., 1994; Goodson & Bass, 2002). The octaval efferent nucleus (OE) projects to the inner ear, which includes the saccule, the main end organ of hearing (Bass et al., 1994, Weeg & Bass, 2000; Weeg et al, 2005). The OE contains reciprocal connections with the VPP (Chagnaud et al., 2011) and receives projections from the PAG (Kittelberger & Bass, 2012; not shown). Nuclei containing 5-HT-ir cells are in red: spinal cord (SC), VMN, AP (area postrema), IRa (inferior raphe), ItRa (intermediate raphe), SRa (superior raphe), PVO (paraventricular organ), Hd (dorsal periventricular hypothalamus), Hc (caudal periventricular hypothalamus), Pit (pituitary), Pr (pretectal nucleus), Ha (Habenula). Red arrows indicate proposed directions and targets of major projection pathways emerging from serotonergic nuclei. The IRa appears to send descending projections to the spinal cord, dorsal processes onto vocal motor neurons (VMN), and dorsal processes to numerous hindbrain nuclei, including hindbrain auditory areas. ItRa appears to send descending processes, likely to spinal cord and hindbrain targets. Projections from SRa are largely ascending and appear to be the likely source of the majority of 5-HT terminals on midbrain and forebrain vocal/auditory areas shown. (b) Drawing depicting the dorsal view of the midshipman brain. Arrow indicates caudal (C) and lateral (L) directions. Letters with lines indicate levels of transverse section images in Figure 2. Scale bar = 2.25 mm [Color figure can be viewed at wileyonlinelibrary.com]

in midshipman. These data will provide important comparative and evolutionary insights on the nature of the serotonergic system in vocal-acoustic communication in vertebrates.

2 | MATERIALS AND METHODS

2.1 | Animals and tissue collection

Animals (n = 56, females = 21, Type I males = 17, Type II males = 18) were either collected by hand from intertidal nest sites in Tomales Bay near Marshall, CA or by trawl in Puget Sound offshore of Edmonds, WA. Prior to perfusion, midshipman were kept in flow-through salt water tanks at the University of California Bodega Marine Laboratory or in recirculating seawater tanks at Aquatic Research and Environmental Assessment Center at Brooklyn College, City University of New York. Animal care and experimental procedures were approved by the Institutional Animal Care and Use Committees of the City University of New York and the University of California.

Experimental animals were anesthetized by immersion in salt water containing 0.25% benzocaine, and perfused with ice-cold teleost Ringer's solution followed by 4% paraformaldehyde in 0.1 M phosphate buffer (PB; pH 7.2). Brains were removed and postfixed for 1 hour in the same fixative and then rinsed and stored in PB + 0.03% sodium azide at 5°C. Prior to sectioning, brains were cryoprotected for 24 hr in PB + 30% sucrose. Tissue was cut at 25 μm in a Leica CM1850 cryostat and resulting sections were adhered to chrome alum gelatin subbed slides or positively charged (superfrost plus) slides. Specimen slides were stored at −80°C until labeled.

2.2 | Immunohistochemistry

Brains from the 56 fish collected were processed with anti-5-HT primary antibody produced in rabbit (#S5545, RRID:AB_477522; Sigma, St Louis, MO) or goat (#20079, RRID:AB_572262; ImmunoStar, Hudson, WI). Alexa Fluor secondary antibodies were used for fluorescence visualization (Thermo Fisher, Waltham, MA). Anti-Hu (#16A11, RRID: AB_2314655; Thermo Fisher) was used in some animals as a neuronal-specific counterstain. Additional colabeling studies with 5-HT were performed with goat choline acetyltransferase (ChAT; #AB144P, RRID:AB_90650), or mouse tyrosine hydroxylase (TH; #MAB318, RRID:AB_2201528) (both antibodies from EMD Millipore, Billerica, MA). IHC was performed at room temperature in the following steps: slides were washed 2 × 10 min in 0.1 M phosphate buffered saline (PBS; pH 7.2), blocked for 1 hr in PBS + 5% donkey serum (DS) + 0.3% Triton-X-100 (PBS + DS + T), incubated with primary antibody diluted in PBS + DS + T for ~18 hr, washed 6 × 10 min in PBS + 0.5% DS, incubated with secondary antibody diluted in PBS + DS + T for 2 hr, washed 5 × 10 min in PBS, 10 min in PBS + 0.01% Triton-X-100, incubated in Neurotrace 500 fluorescent Nissl (Thermo Fisher) for 20 min, washed 3 × 10 min in PBS, and coverslipped with Prolong Gold cover-slipping mounting medium containing DAPI nuclear stain (Molecular Probes, Carlsbad, CA).

2.3 | Neural tract tracing combined with IHC

A subgroup of four Type I males received application of neurobiotin transneuronal tracer (Vector, Burlingame, CA) to the occipital nerve where it connects to the swimbladder vocal musculature (see Forlano, Kim, Krzyminska, & Sisneros, 2014). Postsurgery survival time was 7 days. Tracer IHC protocol followed the outline above but with fluorescent-conjugate streptavidin added for visualization at the secondary step (Molecular Probes).

2.4 | Microscopy

Slides were imaged with an Olympus BX61 epifluorescence microscope using a Hamamatsu ORCA-03G CCD camera and Metamorph software (Molecular Devices, Sunnyvale, CA) for image acquisition. Micrographs for the superior raphe quantitative analyses were imaged using a 20x objective and a multidimensional acquisition method in which five images were acquired at a z-plane thickness of 0.8 μm and stacked using a maximum intensity projection. Manuscript images were compiled, labeled, and level adjusted for contrast in GNU Image Manipulation Program (GIMP). Composite images were assembled using the Adobe Photoshop batch merge utility.

2.5 | Antibody characterization

To verify the specificity of the two anti-5-HT antibodies used in this study: rabbit anti-5-HT (RRID AB:477522) and goat anti-5-HT (RRID: AB_572262), we performed antigen preadsorption tests using 5-HT BSA Conjugate (ImmunoStar, Catalog #20081). Primary antibodies were left in a solution of 125 μg/ml of antigen for ~20 hr at 8°C. Preadsorption eliminated 5-HT-ir label in treated slides but not in control slides containing alternate series from the same animal.

Antigen, manufacturers, RRID, species, and dilutions for all primary antibodies used in this study are listed in Table 1. Recent studies in plainfin midshipman utilizing EMD Millipore goat polyclonal anti-ChAT antibody (Forlano, Ghahramani et al., 2015; Forlano, Sisneros, et al., 2015; Perelmuter & Forlano, 2017) results in labeling matching that found here. Anti-ChAT antibody is produced against whole choline acetyltransferase purified from human placental lysate and western blot analysis shows bands of 68–70 kDa in mouse brain extract (manufacturer's information). Additional western blot analysis shows similar bands of 68–72 kDa in the African clawed frog (López, Perlado, Morona, Northcutt, & González, 2013), lesser spotted dogfish, sturgeon, trout (Anadón et al., 2000), and Senegal bichir (López et al., 2013). The pattern of labeling in the midshipman fish is comparable to that reported in a broad range of nonmammalian vertebrates where the antibody has been well characterized and used to describe

TABLE 1 Primary antibodies used

Name	Immunogen	Manufacturer	RRID	Type	Species	Dilution
Anti-ChAT	Choline acetyltransferase purified from human placenta.	EMD Millipore, #AB144	AB_90650	Polyclonal	Goat	1:200
Anti-5-HT	Serotonin creatinine sulfate complex conjugated with formaldehyde to BSA.	Sigma, #S5545	AB_477522	Polyclonal	Rabbit	1:4,000
Anti-5-HT	Serotonin coupled to BSA with paraformaldehyde.	ImmunoStar, #20079	AB_572262	Polyclonal	Goat	1:400
Anti-Hu	Human HuC/HuD neuronal protein from human.	Thermo Fisher, #16A11	AB_2314655	Monoclonal	Mouse	1:1,000
Anti-tyrosine hydroxylase	Tyrosine hydroxylase purified from PC12 cells.	EMD Millipore, #MAB318	AB_2201528	Monoclonal	Mouse	1:1,000

cholinergic neurons and fibers that are generally conserved across vertebrates (Rodríguez-Moldes et al., 2002). ChAT labels cholinergic cranial motor neurons and nerves, auditory efferent neurons, and fibers in amphibians (Marín, Smeets, & González, 1997), bichir (López et al., 2013), dogfish (Anadón et al., 2000), lamprey (Pombal, Marín, & González, 2001), lizard (Wibowo, Brockhausen, & Köppl, 2009), pigeon (Medina & Reiner, 1994), rainbow trout (Pérez et al., 2000), red-eared turtle (Jordan, Fettis, & Holt, 2015), sturgeon (Adrio, Anadón, & Rodríguez-Moldes, 2000), and zebrafish (Mueller, Vernier, & Wullimann, 2004). Omission of anti-ChAT primary antibody or secondary antibodies results in absence of labeling (Table 2).

The antigen for the mouse monoclonal anti-TH antibody was purified from PC12 cells and western blot analysis of both rat and fish brain lysate show comparable expected bands of 59–63 kDa and no cross-reactivity with other structurally similar enzymes (Adrio, Anadón, & Rodríguez-Moldes, 2002; Goebrecht, Kowtoniuk, Kelly, & Kittelberger, 2014; manufacturer's information). Anti-TH label is consistent with findings of catecholaminergic neurons and fibers in plainfin midshipman (Forlano et al., 2014; Ghahramani et al., 2015; Goebrecht et al., 2014; Perelmuter & Forlano, 2017), other teleosts (McLean & Fetcho, 2004; Tay, Ronneberger, Ryu, Nitschke, & Driever, 2011) and across vertebrates (Smeets & González, 2000; Xavier et al., 2017). Omission of anti-TH antibody in parallel series control trials resulted in an absence of labeling.

Sigma anti-5-HT is raised in rabbit against serotonin creatinine sulfate complex conjugated to BSA (manufacturer's information) and labels 5-HT-ir neurons in the raphe formation of all vertebrates. The manufacturer reports no cross-reaction with L-tryptophan, 5-HTP, *N*-acetylserotonin, or dopamine at a concentration of 500 μM and inhibition of staining in rat brain by preincubation of antibody with 200 μg/ml serotonin-BSA. It has been used previously in numerous studies in fish, including zebrafish (Kuscha, Barreiro-Iglesias, Becker, & Becker, 2011), African cichlid (Whitaker et al., 2011), and Mexican tetra (Dufton, Hall, & Franz-Odendaal, 2012), and other vertebrates including African clawed frog, chicken (Xavier et al., 2017), and mouse (Cohen, Amoroso, & Uchida, 2015).

Immunostar anti-5 HT is raised in goat against serotonin coupled to BSA with paraformaldehyde (manufacturer's information) and labels 5-HT-ir neurons in the raphe formation of all vertebrates. The manufacturer reports labeling is eliminated in rat hypothalamus and spinal cord by pretreatment of antibody with 100 μg of serotonin/BSA conjugate. It has been used in, among other vertebrates, zebrafish (Olsson, 2011), bullfrog (Reyes, Fong, Brink, & Milsom, 2014), rat (Yin et al., 2014).

The antigen for anti-Hu, used to label differentiated neurons, was isolated from human tissue in a patient with paraneoplastic encephalomyelitis and has been utilized in midshipman (Forlano, Deitcher, Myers, & Bass, 2001) zebrafish, African clawed frog, and chicken (Xavier et al., 2017), among other vertebrates. Omission of anti-Hu antibody in parallel series control trials resulted in an absence of labeling.

2.6 | Quantification of cell mophometrics

Animals collected from nests (n = 16, Type I males = 7, Type II males = 9, standard length range = 7.7–19.6 cm, 2nd and 3rd quartiles = 10.9, 16 cm) were utilized to test the hypothesis of subregional morphometric heterogeneity in the serotonergic superior raphe.

Landmark-based boundaries for three superior raphe subregions were assigned (see Superior raphe results section for anatomical sampling details). An observer blind to the goals of the experiment identified and counted all cells that fell within each zone per animal in a sample of evenly-spaced transverse sections corresponding to 1/8 of SRa sections with 5-HT-ir somata present. Sampled sections were thus approximately 171 μm apart (adjusting for maximum intensity z-stack projection thickness of ~4 μm) and sufficiently separated to preclude the possibility of double counts. A 5-HT-ir cell would only be counted if it contained and surrounded a DAPI labeled nucleus. For each animal analyzed, a proportional sample of cells per section was randomly assigned for perimeter tracing of 5-HT-ir somata, thus generating area and mean intensity data for quantitative analysis. The above tracing proportion was derived as follows: in each section, if the number of cells counted and assigned to a subregion was greater than 1 but less than-or equal to 7, one cell was randomly selected and measured; If greater than 7 but less than-or-equal to 12, two cells were measured; >12 and ≤18, three were measured, and >18, four cells were measured. Image counts, cell tracing, and area/intensity

TABLE 2 Neuroanatomical abbreviations

ac	Anterior commissure
AP	Area postrema
AT	Anterior tuberal nucleus
c	Cerebellar commisure
CA	Cerebral aqueduct
Cb	Cerebellum
cc	Cerebellar crest
Cg	Granular layer of the corpus of the cerebellum
Cm	Molecular layer of the corpus of the cerebellum
CP	Central posterior nucleus of the thalamus
d	Descending octaval nucleus
d	Dorsal subregion of SRa
D	Area dorsalis of the telencephalon
Dc	Central zone of D
Df	Diffuse nucleus of the hypothalamus
DH	Dorsal horn
dl	Dorsolateral division of d
Dl	Lateral zone of D
Dld	Dorsal zone of Dl
Dlv	Ventral zone of Dl
dm	Dorsomedial division of d
Dm	Medial zone of D
Dm-cm	Central medial zone of Dm
Dm-p	Posterior zone of Dm
Dp	Posterior zone of D
DPo	Dorsal posterior nucleus of the thalamus
EG	Eminentia granularis
G	Nucleus glomerulosus
Ha	Habenula
HaB	Habenular commisure
Hc	Caudal periventricular hypothalamus
Hd	Dorsal periventricular hypothalamus
HoC	Horizontal commissure
Hv	Ventral periventricular hypothalamus
iaf	Internal arcuate fiber tract
IIn	Optic nerve
III	Third ventricle
IIIn	Oculomotor nerve
IL	Inferior lobe of the hypothalamus
IP	Isthmal paraventricular nucleus
IRa	Inferior raphe
Is	Isthmal nucleus (not nucleus isthmi)
ItRa	Intermediate raphe
IV	Fourth ventricle
IX	Glossopharyngeal nerve
LC	Locus coeruleus
LHa	Left habenula
ll	Lateral lemniscus
lr	Lateral recess
MFB	Medial forebrain bundle
MLF	Medial longitudinal fasiculus
NIn	Interpeduncular nuclei
nll	Nucleus of the lateral lemniscus
NLV	Lateral nucleus of the valvula
nMLF	Nucleus of the MLF
OB	Olfactory bulb
OE	Octavolateralis efferent nucleus
OEc	Caudal division of OE
OEr	Rostral division of OE
Omc	Oculomotor complex
OT	Optic tract
PAG	Periaqueductal gray
Pe	Periventricular cell layer of the midbrain tectum
PGl	Lateral division of nucleus preglomerulosus
PGm	Medial division of nucleus preglomerulosus
PHT	Preoptico-hypophysial tract
Pin	Pineal
PinS	Pineal stalk
Pit	Pituitary
PL	Paralemniscal midbrain tegmentum
PLLn	Posterior lateral line nerve
PM	Magnocellular preoptic nucleus
PMg	Gigantocellular division of PM
PoC	Posterior commissure
PPa	Anterior parvocellular preoptic nucleus
PPp	Posterior parvocellular preoptic nucleus
Pr	Pretectal nucleus
PTN	Posterior tuberal nucleus
PTT	Paratoral tegmentum
PVO	Paraventricular organ
RF	Reticular formation
RHa	Right habenula
s	Sulcus
Sac	Saccule
sac	Stratum album centrale
SC	Spinal cord
sfgs	Stratum fibrosum et griseum superficiale
sgc	Stratum griseum centrale
slat	Lateral sulcus
SCN	Suprachiasmatic nucleus
SD	Saccus dorsalis
SE	Sensory epithelium of the saccule
SM	Supramedullary neurons
Sn	Spinal nerve

TABLE 2 (Continued)

SOv	Ventral division of secondary octaval nucleus
SRa	Superior raphe
SRa-d	Dorsal subregion of SRa
SRa-vl	Ventrolateral subregion of SRa
SRa-vm	Ventromedial subregion of SRa
SV	Saccus vasculosus
T	Telencephalon
TD	Torodiencephalic bundle
TeM	Midbrain tectum
TL	Torus longitudinalis
TPp	Periventricular posterior tuberculum
TS	Torus semicircularis
Vn	Trigeminal nerve
V	Area ventralis of the telencephalon
VIIn	Facial nerve
v	Ventricle
Vc	Central nucleus of V
Vd	Dorsal nucleus of V
Vde	Descending tract of the trigeminal nerve
Vg	Granular layer of the valvula
VH	Ventral horn
VI	Abducens motor nucleus
VIc	Caudal division of VI
VIr	Rostral division of VI
VIIIn	Eighth nerve
VIIm	Facial motor nucleus
VIn	Abducens ascending tracts
VII	Facial tract
vl	Ventrolateral subregion of SRa
vm	Ventromedial subregion of SRa
Vm	Molecular layer of the valvula
VM	Ventromedial nucleus of the thalamus
VMN	Vocal motor nucleus
Vp	Postcommissural nucleus of V
VPN	Vocal pacemaker nucleus
VPP	Vocal prepacemaker nucleus
Vs	Supracommissural nucleus of V
VT	Ventral tuberal hypothalamus
Vv	Ventral nucleus of V
XL	Vagal lobe
IXn	Glossopharyngeal nerve
Xm	Vagal motor nucleus
Xn	Vagus nerve
y	Sulcus ypsiloniformis

measurements were performed in the ImageJ (Schindelin, Rueden, Hiner, & Eliceiri, 2015) using the "Custom Macros" plugin (Timothy & Forlano, 2019). Specifically, the "Manual Cell Count" module of the plugin was used for cell counts and "Area Measurement" module (without thresholding) for cross-sectional area.

2.7 | Statistics

One-way repeated measures ANOVA tests were used to compare the three superior raphe subregions within animals in relation to: (a) cell counts, (b) cross-sectional of traced cells, (c) average intensity of traced cells. Mauchly's test was used to determine sphericity prior to ANOVA and the Holm–Bonferroni method was utilized for posthoc analysis between subregions. Data were compiled in LibreOffice Calc (The Document Foundation; Berlin, Germany), and statistical analyses performed in JASP (The JASP Team, 2019). Graphs were generated using the GraphPad Prism (La Jolla, CA) and laid out in GIMP.

3 | RESULTS

3.1 | 5-HT-ir cell groups

3.1.1 | Overview

The majority of serotonergic efferents in the teleost brain are located in the periventricular hypothalamus and the brainstem reticular formation. Additional cell populations are found in the pretectum, the epithalamus, pituitary, and area postrema (AP). Significantly, the cytoarchitectural and projection characteristics of neurons in the hypothalamus are distinct from those in the brainstem and pretectum, with the former being csf-contacting neurons and the latter being classical interneurons. The brainstem populations of 5-HT neurons are found throughout much of the medial rhombencephalon, with dense clusters in the isthmus and ventral caudal medulla. Most of these neurons are found within the raphe of the reticular formation.

The rostral-caudal distribution of 5-HT neuronal populations is outlined below, with corresponding atlas images from Figures 1b and 2 in parentheses, and are referred to in schematic 1a:

Pineal organ (Pin; 2f), habenula (Ha; 2f), paraventricular organ (PVO; 2f), dorsal periventricular hypothalamus; (Hd; 2f-g), caudal periventricular hypthalamus (Hc; 2f-h), pretectal nucleus (2g), superior raphe (SRa; 2i-K), intermediate raphe (ItRa; 2l), ventrolateral reticular formation (RF; double headed arrow in 2n), inferior raphe (IRa; 2o-r), area postrema (AP; 2q). Subregions of the SRa and IRa are described in detail in the section on serotonergic brainstem populations.

Horizontal and sagittal views of cell groups are supplied in Figures 3 and 4, respectively. The pituitary also contains numerous 5-HT-ir cells (see Figure 5a).

3.1.2 | Pretectal nucleus

The pretectal nucleus (Pr; Figures 2g and 4a,g) is composed of bilateral columns of ovoid 5-HT-ir somata directly lateral to the third ventricle

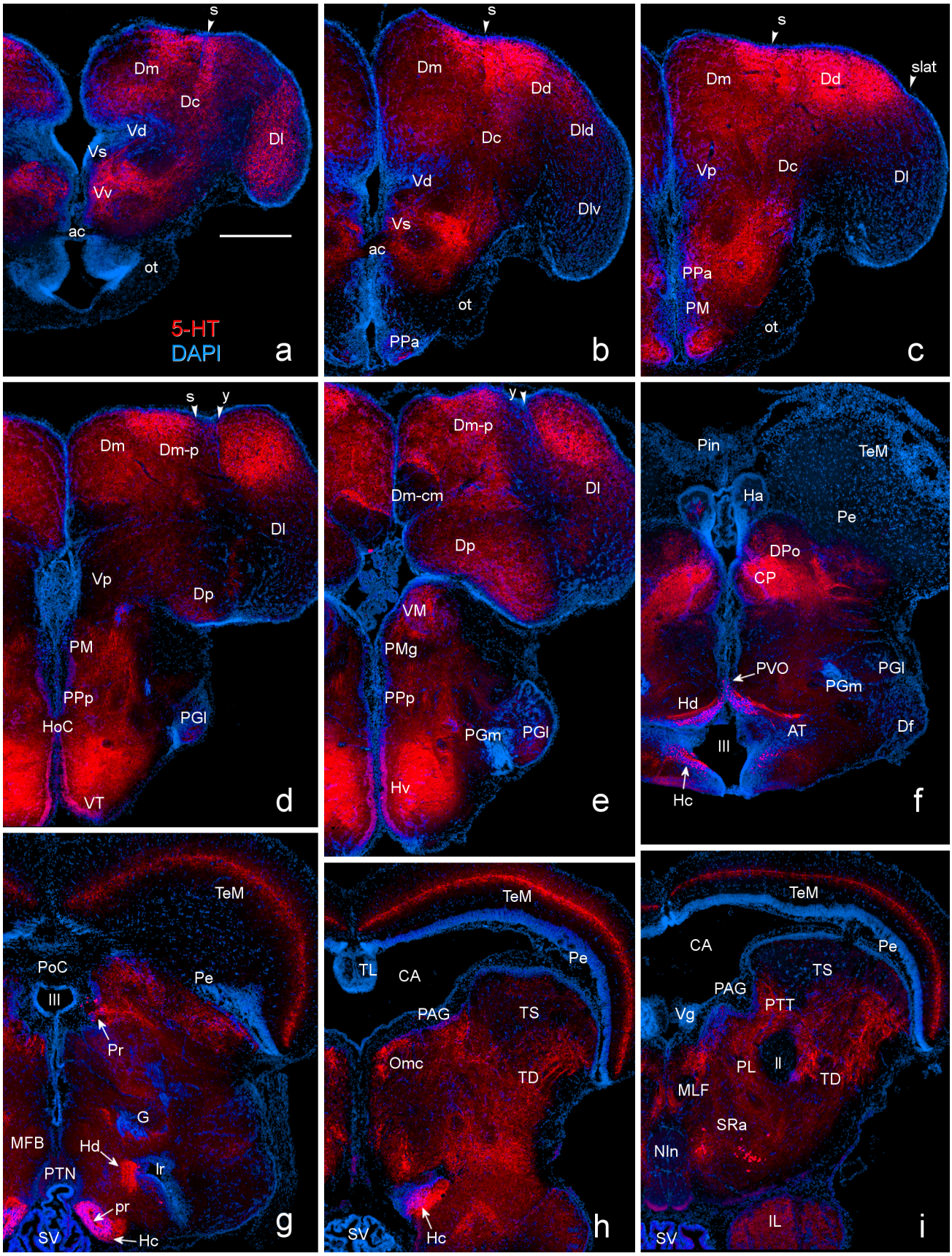

FIGURE 2 Atlas of rostrocaudal distribution of serotonergic immunoreactivity (5-HT-ir) in red in the transverse plane. Letters match cross-sections indicated in Figure 1b. Blue is DAPI. Scale bar = 250 μm [Color figure can be viewed at wileyonlinelibrary.com]

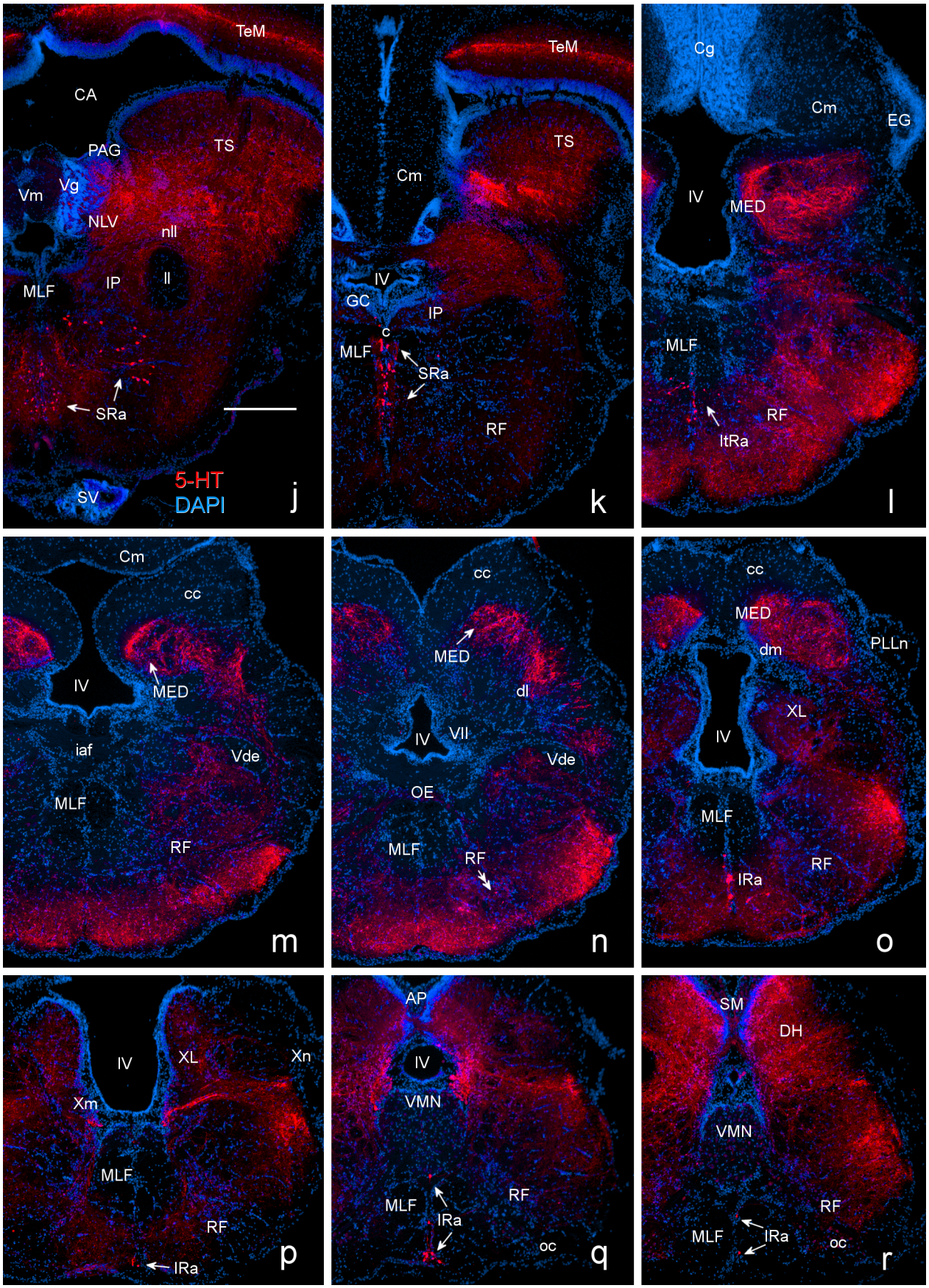

FIGURE 2 (Continued)

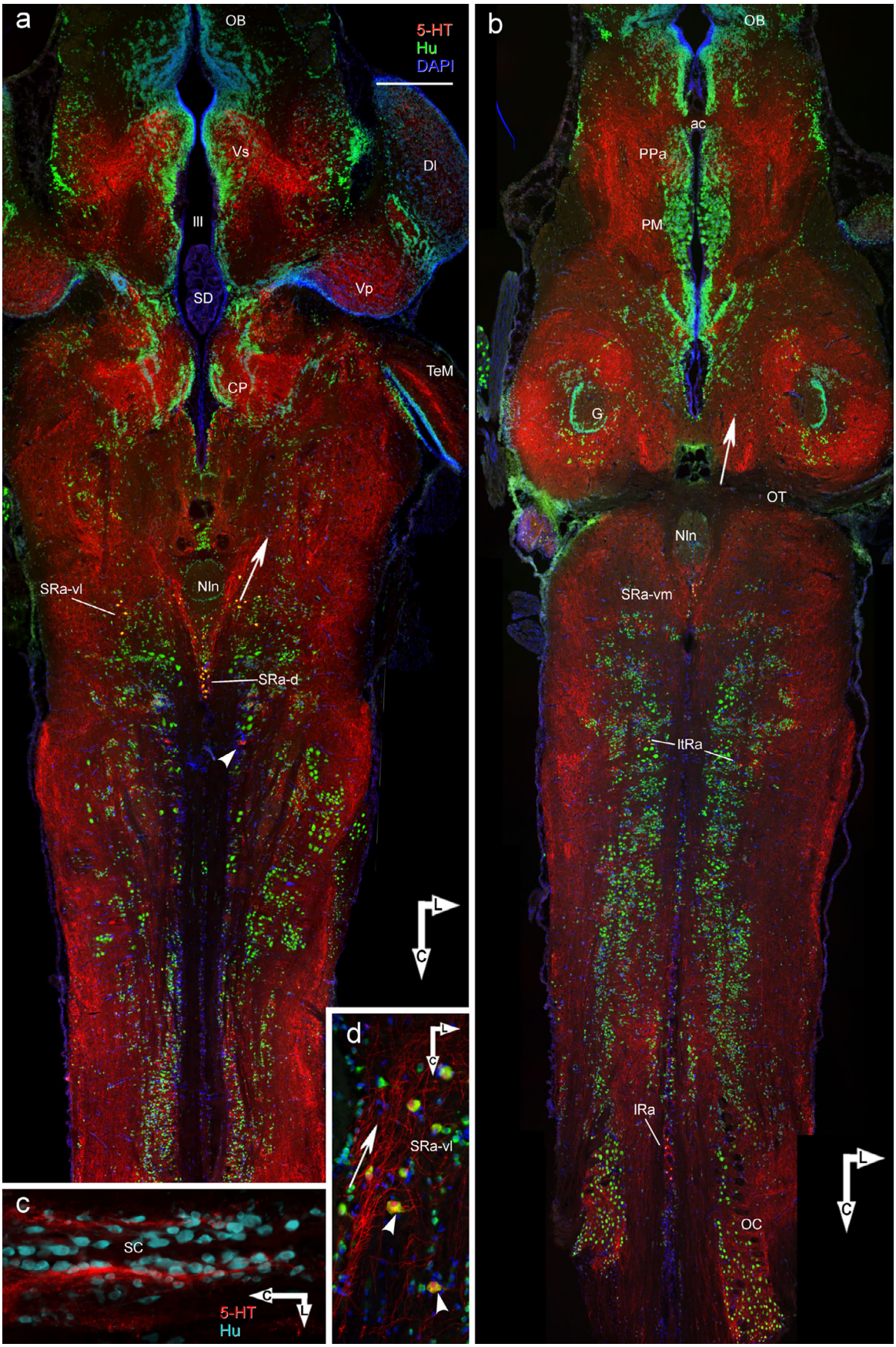

FIGURE 3 Legend on next page.

and extending longitudinally. The most rostral Pr cells are found ventral to the habenula (Ha), dorsal to the central posterior nucleus, and dorsomedial to the dorsal posterior nucleus of the thalamus (DPo; Figure 2f). The Pr is ventrolateral to the posterior commisure (PoC), and terminates caudally near the commisure's posterior boundary. Cell bodies lie adjacent to the perimeter of the fasciculus retroflexus, a habenular efferent tract identifiable through ChAT-ir, a cholinergic marker, and devoid of 5-HT-ir (Timothy and Forlano, unpublished observations). Processes arising from the Pr are conspicuously unidirectional, gradually tapering in thickness in ipsilateral projections putatively terminating in the midbrain tectum. The habenula does not appear to receive 5-HT-ir fibers from the Pr, despite the proximity of these areas.

3.1.3 | Hypothalamic nuclei

We have adopted our nomenclature from Rink and Wullimann (2001) to describe the regional anatomy of the midshipman serotonergic hypothalamic populations and identified each region based on the part of the diencephalic/third ventricular system (III) with which it borders. We found an extensive and dense population of cerebral spinal fluid (csf)-contacting 5-HT-ir neurons in the midshipman periventricular hypothalamus. The most caudal hypothalamic 5-HT-ir cells are in a tight circular cluster surrounding the posterior recess of the third ventricle (pr, Figures 2g and 4a) in the caudal periventricular hypothalamus (Hc; Figures 2f,g and 4a). Moving rostrally, the posterior recess opens into the ventral region of III and the lateral recess (lr). Hc neurons are also found ventromedial to lr. 5-HT neurons in the dorsal periventricular hypothalamus (Hd; Figures 2f,g and 4a,i,j) are associated with proximity to the lateral recess. Again moving rostrally, III opens into a triangular wedge shape pointing dorsally and is bound laterally by the most rostral hypothalamic 5-HT-ir cells of the PVO(Figures 2f and 4h). These neurons appear somewhat continuous with Hd but are in a more dorsomedial orientation and are associated with a narrowing of the rostral III (Figures 2f and 4i).

All hypothalamic 5-HT cells contain thick cytoplasmic processes that extend medially to the ventricular surface (arrow in Figure 4h). Fine varicose processes emerge laterally at the other pole of these cells coalescing in very dense tracts that appear to terminate locally (Figure 4h). Some of these processes contain swellings contacting dendrites and cells bodies of co-regional dopaminergic neurons in the periventricular posterior tuberculum (TPp; carets in Figure 4h). Interestingly, hypothalamic 5-HT-ir cells do not colocalize with the neuronal specific marker Hu (Figure 4j), despite the clearly neuronal morphology of these cells, matching recent data from chicken, african clawed frog, zenopus, and zebrafish (Xavier et al., 2017).

3.1.4 | Pituitary

5-HT-ir cells are found throughout the midshipman pituitary (Pit). We identified 5-HT-ir cells in pars nervosa and pars distalis. The somata are irregularly shaped and contain short cytoplasmic processes from which emerge fine fibers that project locally in the pituitary (Figure 5a).

3.1.5 | Epithalamus

We identified 5-HT-ir somata in the midshipman pineal vesicle (Pin; Figure 5b). Clusters of cells in the pineal show both 5-HT-ir and ChAT-ir. Interestingly, the midshipman basal pineal stalk (PinS) does not contain 5-HT-ir or ChAT-ir.

5-HT-ir labeling in the habenula appears highly variable between animals. Some individuals show numerous small round 5-HT-ir cells lacking visible processes in the dorsal habenula (Figure 5c). Staining in these cells has a crescent-like appearance, owing to the relatively small 5-HT-ir cytoplasmic space compared to the (unlabeled) nucleus. Presence of 5-HT neuronal labeling is pronounced in the caudal habenula and is sparse at the rostral extent of the habenula. Interestingly, some animals sampled had very few, or no habenular 5-HT-ir cells.

3.1.6 | Raphe formation

Superior raphe

The superior raphe (SRa) contains the majority of ascending 5-HT projection neurons in the brain (Figures 2i–K, 3a,b,d, 4a,f, and 6a–f). Examination of the midshipman SRa suggests heterogeneity of 5-HT cell groups within this region. Based on the location of 5-HT-ir neurons relative to anatomical landmarks and subsequent quantitative analysis, we identified three superior raphe subnuclei: SRa-d (dorsal subregion), SRa-vm (ventromedial subregion), and SRa-vl (ventrolateral subregion). The topographical demarcation of these regions was done utilizing the following boundary axes: (a) A "ventral medial longitudinal fasciculus (MLF) axis"

FIGURE 3 5-HT-ir (red) in the horizontal plane. Arrows indicate caudal (C) and lateral (L) directions. (a) Composite view, cut at a mid-frontal plane showing the dorsal subregion of the superior raphe (SRa-d) with with its ascending fiber projections (arrow) and the ventrolateral subregion of the superior raphe (SRa-vl). Note two prominent regions of 5-HT-ir at this level are the terminal fields in the ventral telencephaic supracommissural nucleus (Vs) and the thalamic central posterior nucleus (CP). (b) Composite view ventral to that in a. Note the ascending 5-HT-ir fibers (arrow) rostral to the optic tract (OT). The cells of the intermediate raphe (ItRa) can be found in two columns lateral to the MLF. (c) High magnification view of two longitudinal 5-HT tracts in the ventral floor of the spinal cord (SC). Orientation is rotated clockwise 90° relative to figures a and b. (d) Ascending fibers from SRa-d (arrow, as in a). Laterally facing processes extending from SRa-vl cells are indicated with carets. Green is Hu-ir, blue is DAPI and teal is Hu-ir in c. Scale bars = 500 μm in a, B; 100 μm in c, d [Color figure can be viewed at wileyonlinelibrary.com]

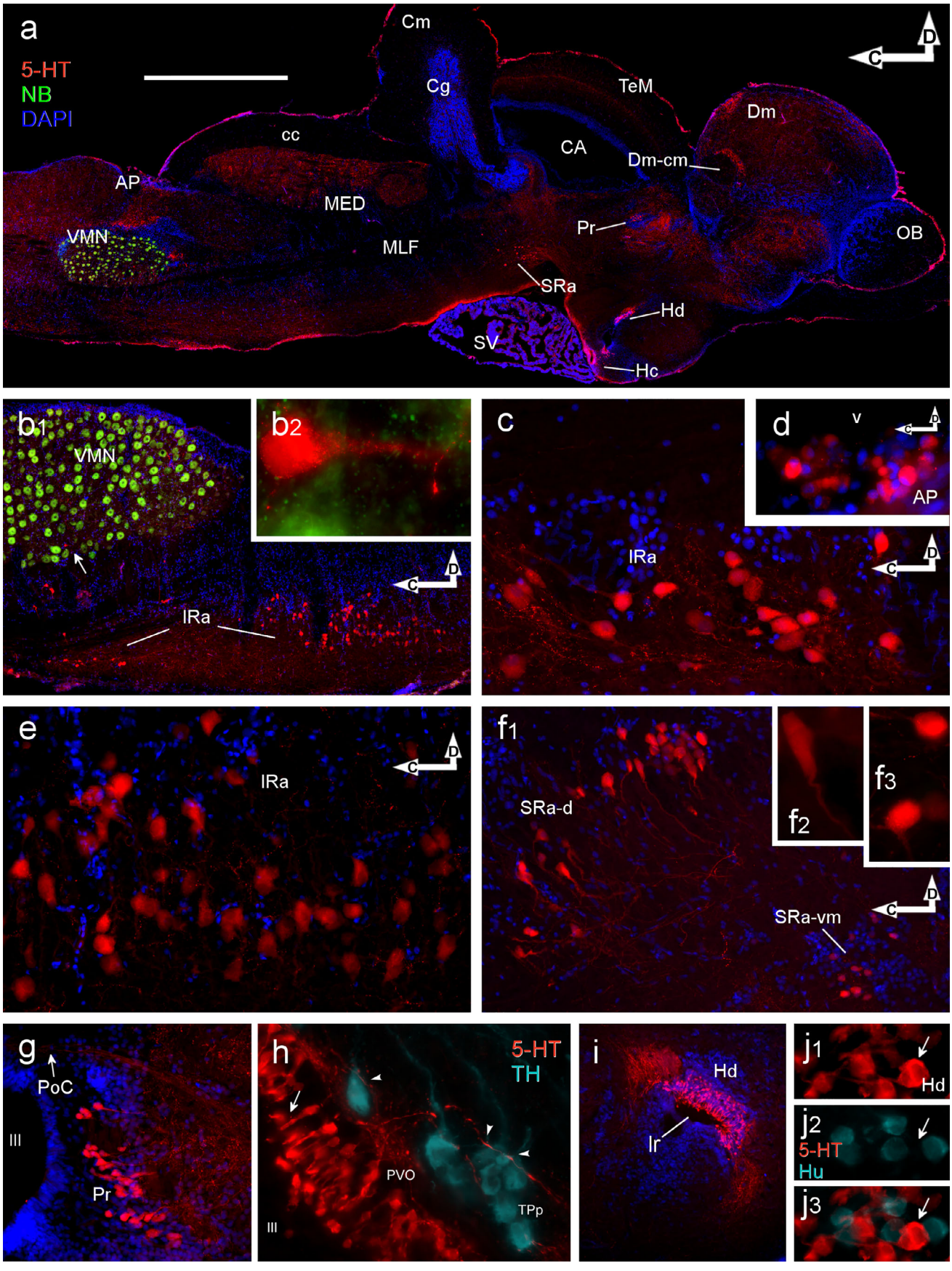

FIGURE 4 Legend on next page.

(Figure 6b,c; horizontal dotted line) situated just below the ventral base of the MLF, (b) Two "lateral MLF axes" situated at the distal boundaries of the MLF (Figure 6c, vertical dotted lines), (c) A boundary drawn around the periphery of interpeduncular nuclei and the region immediately posterior to it (NIn; Figure 6c, rounded rectangular dotted trace).

The most rostral cells in SRa are found in SRa-vl located at the ventrolateral midbrain/hindbrain boundary and are relatively diffuse at their most rostral extent having no definitive rostral landmark cut-off. In contrast, the caudal superior raphe has an abrupt caudal boundary near the cerebellar commisure (c; Figure 2k). Due to this condition, the clearest way to describe the morphology of the SRa groups is starting at their posterior-most extent and moving anteriorly.

SRa-d

Starting at the caudal boundary of the isthmus, cells appear in an elongated cluster at the midline and continue rostrally along the midline with somata being found between and also overlapping the MLF (Figures 2k and 6a–c). All 5-HT-ir neurons dorsal to the "ventral MLF axis" are in the SRa-d group (Figure 6b,c). Some of the more rostral SRa-d cells are found ventrolateral to the "ventral MLF axis" but always outside of the NIn boundary (Figure 6c). The resemblance of cerebellar commisure (c) as a dorsal/median raphe boundary appears to be a superficial one and we group cells dorsal and ventral to c in SRa-d. Cells in SRa-d are relatively fusiform and send mostly unidirectional ascending processes that fan out around the NIn (Figures 3a,d, 4f1,f2, and 6a–c,e).

SRa-vm

Approximately 300–400 μm rostral to the first appearance of SRa (depending on brain size and plane of section), a group of distinct, medial cells ventral to the "the ventral MLF axis" emerge. These somata are separated at the midline from SRa-d by an interruption of 5-HT-ir but not neuronal (Hu-ir) somata (Figure 6b). More rostrally, SRa-vm cells occur within and along the periphery of the NIn (Figure 6c). These neurons generally appear distinct from 5-HT-ir neurons outside the NIn boundary in being distinctly ovoid and significantly smaller than cells in SRa-d and SRa-vl (Figures 4f, 6f, and 7). They are multipolar and contain ascending processes (Figures 4f1,f3 and 6f).

SRa-vl

This is the most rostral brainstem serotonergic population and is found in a distinctly lateral placement (Figures 3a and 6c) compared to the closely medial location of the other raphe neurons (with the exception of the relatively lateral and diffuse intermediate raphe (ItRa; Figure 6g) and ventrolateral reticular formation group (RF; Figure 6h). SRa-vl appears just rostral to the plane that the SRa-vm group enters and continues rostrally until ending near the mesencephalic tegmentum. SRa-vl neurons are ventrolateral to MLF. Cells in SRa-vl are comparatively large and their somata display the greatest average area in the SRa (Figure 7). Some of the most lateral cells in this group are distinctly fusiform exhibiting bipolar proximal processes that are laterally bidirectional (Figure 6d).

Quantitative morphometric analysis of superior raphe subregions

One-way repeated measures ANOVA tests were used to assess the three superior raphe subregions within animals in relation to: (a) cell count, (b) cross-sectional area of traced cells, (c) average intensity of traced cells. Mauchly's test validated the assumption of sphericity for all three measures ($p > .5$). Results indicated significant variation in cell count, ($F_{(2, 30)} = 20.06$, $p < .001$) and cross-sectional cell area, ($F_{(2, 30)} = 50.18$, $p < .001$) between SRa subregions. No significant differences were found in average intensity ($F_{(2, 30)} = 1.766$, $p = .188$). Post-hoc analyses were performed on cell count and area metrics using the Holm–Bonferroni method and confirmed significant differences in comparisons between subregions (Figure 7).

Intermediate raphe

We identified a distinct population of 5-HT-ir neurons in an intermediate raphe population in the dorsorostral reticular formation (ItRa;

FIGURE 4 Sagittal views of 5-HT-ir (red) in hindbrain (a–f) and transverse views of forebrain 5-HT-ir cell groups (g–j). Blue is DAPI. Arrows indicates caudal (C) and dorsal (D) directions in sagittal sections. (a) Mid-sagittal view of the brain with backfilled vocal motor nucleus (VMN) in green (Neurobiotin—NB). (b1) Parasagittal view of the brain with backfilled VMN in green. Arrow points to a 5-HT-ir cell in the vocal motor nucleus (VMN). (b2) High magnification view of 5-HT-ir cell indicated by arrow in b1 and located within the boundaries of the VMN. The rostrocaudal extent of the inferior raphe (IRa) is indicated. Note that the IRa contains a caudal population, ventral to the VMN, and close to the base of the brain, and a rostral group, to the right of the figure. (c) Sagittal view of the caudal IRa described in b. Note the bipolar longitudinal processes of these cells. (d) Sagittal view of the serotonergic area postrema (AP). These minute cells appear to comprise the smallest 5-HT-ir cell population in the midshipman brain, in terms of both cell number and size. (e) Sagittal view of the rostral IRa population described in b. 5-HT-ir neurons in this population exhibit a different proximal process directionality compared with the caudal IRa. Proximal processes appear to be mostly dorsoventral rather than longitudinal as in caudal IRa. (f1) Mid-sagittal view of the superior raphe (SRa). The cells of the dorsal subregion of SRa (SRa-d) are in the upper left and the ventromedial subregion of SRa (SRa-vm) are in the lower right. Note the larger size and more pronounced directionality of SRa-d. (f2) Sagittal, high magnification view of SRa-d neurons. Note the fusiform shape and unidirectional process. (f3) Sagittal, high magnification view of SRa-vm neurons. Note the ovoid shape. (g) Transverse plane view of pretectal 5-HT-ir group (Pr) in the dorsal thalamus. Arrow points to 5-HT-ir fiber decussation at the posterior commisure (PoC). (h) Transverse plane view of the hypothalamic 5-HT-ir cells of the paraventricular organ (PVO). Arrow points to cytoplasmic process extending to the third ventricle (III) from one of these csf-contacting neurons. Carets indicate putative contacts on dopaminergic (TH-ir, teal) periventricular posterior tuberculum (TPp) neurons. (i) Transverse plane view of 5-HT-ir cells in the dorsal periventricular hypothalamus (Hd) with dense fibers originating from these cells. (j1-3) High magnification transverse plane view of neurons in the caudal periventricular hypothalamus (Hd) showing lack of overlap with neural-specific Hu-ir signal (teal).Scale Bar = 1.8 mm in a; 667 μm in b1; 35 μm in b2; 133 μm in c; 70 μm in d; 133 μm in e; 200 μm in f1; 70 μm in f2, f3 [Color figure can be viewed at wileyonlinelibrary.com]

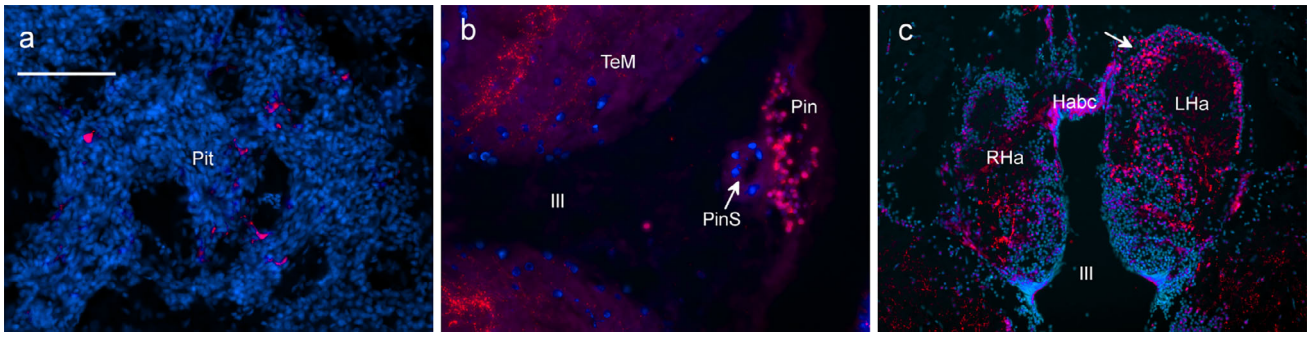

FIGURE 5 5-HT-ir (red) cells in pituitary, pineal and habenula. (a) Transverse views of pituitary (Pit). 5-HT-ir cells have an irregular morphology with only locally extending processes. Blue is DAPI. (b) Horizontal view of the pineal gland (Pin) and basal pineal stalk (PinS). Blue is Hu. (c) Transverse view of both hemispheres of the left and right habenulae (LHa, RHa) showing 5-HT-ir cell populations. Note asymmetry of Ha. Blue is DAPi. Scale bar = 100 μm in a, B; 200 μm in c [Color figure can be viewed at wileyonlinelibrary.com]

Figures 2l, 3b, and 6g). This population consists of clusters of cells ventrolateral to the MLF in a region rostral and directly lateral to very large reticular neurons and dorsal to the rostral abducens nucleus. We conclude that these neurons are the most rostral members of the inferior raphe; however, due to their distance from other IRa cells and their similarity in size to SRa but not IRa, we define these cells as the intermediate raphe population. Unlike the majority of brainstem raphe cells, notably SRa-d, SRa-vm and the IRa, ItRa neurons are not confined to the midline but rather are interspersed in bilateral clusters, though some scattered cells are found at the midline.

Inferior raphe

Our observation of the midshipman inferior raphe suggests heterogeneity both in the anatomical clustering of IRa populations as well as differential morphology of neurons in these subregions. A ventromedial population of 5-HT-ir cells is visible continuously in serial sections running rostrally from the spinal cord-hindbrain boundary from approximately the longitudinal core of the VMN to the rostral medullar reticular formation just caudal to and ventral of the VIIm (Figures 4b1,c,e and 6h). Heterogeneity exists between the rostral and caudal regions of the IRa (Figures 4b1 and 8c,d); cells in the caudal IRa tend to be clustered near the base of the brain (Figure 8a), with many cells having thick bipolar proximal processes projecting longitudinally (Figure 4c). Some caudal IRa cells are found more dorsally, situated between the MLF and appear to send dorsal projections. The more rostral IRa neurons (Figure 4e) are situated in a seam along the midline and send dorsal projections that appear to continue ipsilaterally, after which they turn and descend in lateral columns.

Ventrolateral reticular formation

Lateral to the IRa are clusters of 5-HT-ir neurons near the ventrolateral periphery of the hindbrain in the intermediate and caudal reticular formation (RF; double arrow in Figure 2n and 6h). This population is more diffuse than the IRa and appears to send descending projections.

Area postrema

The midshipman AP is found in the dorsomedial periventricular medulla rostral to the supramedullary neurons (SMs) and caudal to the dorsal opening of the fourth ventricle. AP contains a population of very small, ovoid 5-HT-ir somata (at the level of Figures 2q and 4a,d). Interestingly, the 5-HT-ir cells of the midshipman AP do not appear to possess any overt process morphology.

Vocal motor nucleus

A small but not insubstantial number of 5-HT-ir neurons (roughly 15–30 cells, pending systematic counting) are interspersed throughout the longitudinal and dorsoventral extent of the midshipman VMN (arrow in Figures 4b1,b2, arrow in 8a1,a2,e). These cells have a multipolar morphology and lack distinct projection directionality. Moreover, they appear smaller than the IRa neurons located in the adjacent ventral hindbrain/ spinal cord boundary. Processes arising from 5-HT-ir cells located within VMN make putative contacts onto nearby VMN somata and dendrites (carets in Figure 8e).

Spinal cord

After a gap near the caudal VMN, 5-HT-ir neurons are found in the ventral spinal cord. These cells are mostly ventromedial and resemble those in the caudal ventromedial IRa in location and morphology. Most spinal 5-HT-ir cells send thick descending axons in the medial column of the ventral spinal cord (Figure 9g1,g3). As in the medulla, some 5-HT-ir cells are also found in a ventrolateral region and may send projections in more lateral columns in the spinal cord.

3.2 | 5-HT-ir fibers

3.2.1 | Overview

Serotonin-ir fiber distribution in midshipman is widespread but quite heterogeneous, reflecting likely specialization of targets for 5-HT action. Moreover, we observed significant 5-HT-ir in vocal-acoustic complexes relevant in our behavioral model. Several higher order

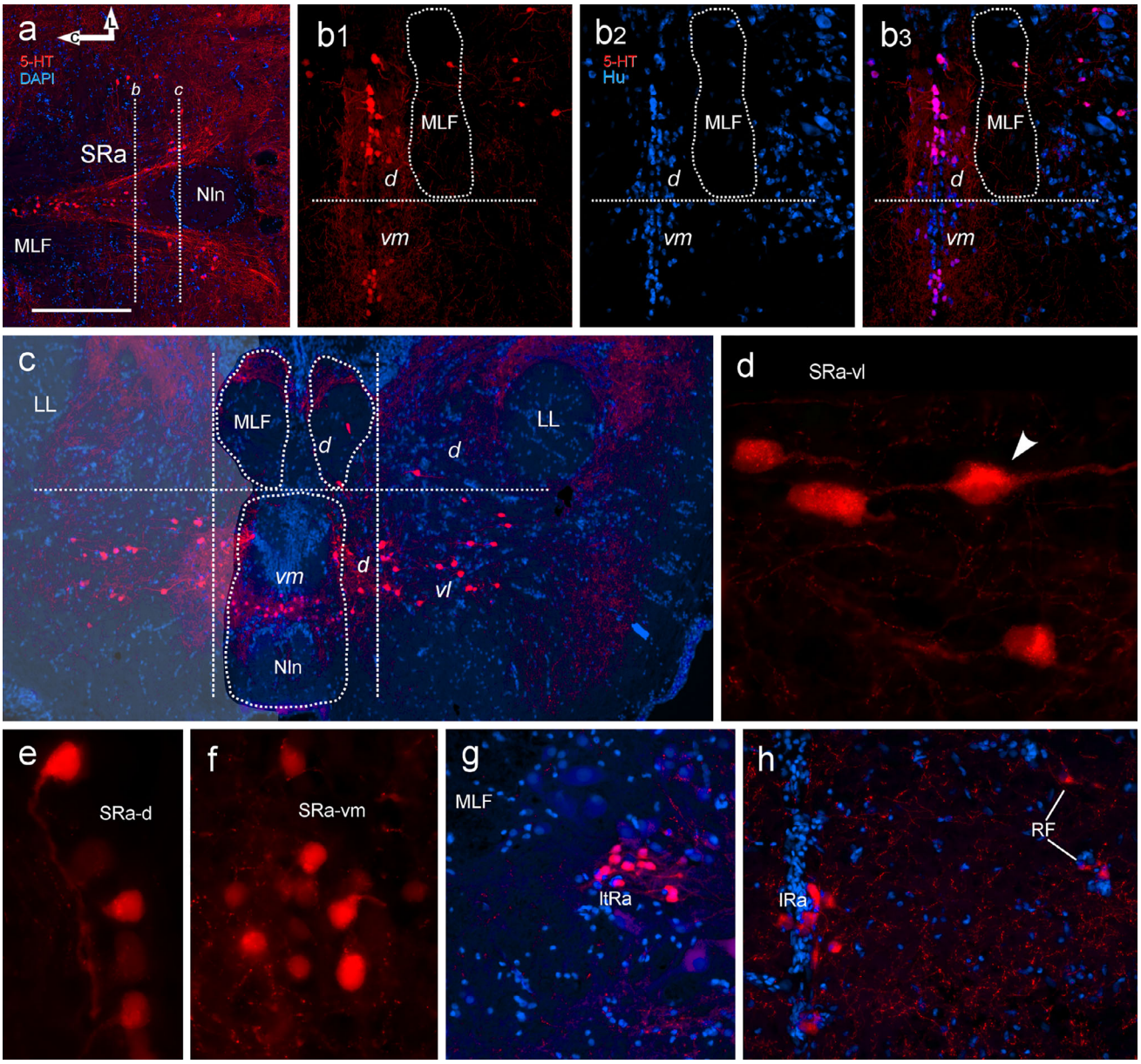

FIGURE 6 Raphe groups. 5-HT-ir in red. Blue is DAPI in all sub-figures except b2-3, in which it is Hu-ir. (a) Midshipman superior raphe (SRa) in the horizontal plane. Arrow indicates caudal (C) and lateral (L) directions. Note the dense, highly directional rostral projection pattern of processes arising from the medial 5-HT-ir cells. Dotted vertical lines, from left to right, represent transverse locations of figures b1-3 and C, respectively. (b) Transverse view of the caudal SRa indicating dorsal (SRa-d) and ventromedial (SRa-vm) subregions. Only the italicized suffixes are shown (*d*,*vm*). (b1) 5-HT-ir only. (b2) Hu-ir only. (b3) 5-HT-ir and Hu-ir overlaid. The dotted horizontal line marks the "ventral MLF boundary" separating cells in SRa-d (above the line) and SRa-vm (below the line). Note that although there is a distinct absence of 5-HT-ir cells at the SRa-d/SRa-vm boundary, non-5-HT-ir neurons are found uninterrupted along the midline (as indicated by blue Hu label). (c) Transverse image of brain section containing all three raphe subregions: dorsal (SRa-d), ventromedial (SRa-vm), and ventrolateral (SRa-vl). Only the italicized suffixes are shown (*d*, *vm*, and *vl*). Gray overlay indicates area not sampled during morphometric analyses. The medial longitudinal fasciculus (MLF) is indicated by two dotted horizontal ovals. The topographical demarcation of these regions utilizes three axes: (a) A "ventral MLF axis" (horizontal dotted line) situated just below the ventral base of the MLF, (b) Two "lateral MLF axes" situated at the distal boundaries of the MLF (vertical dotted lines), (c) A boundary drawn around the periphery of the interpeduncular nuclei and the region immediately posterior to it (NIn; rounded rectangular dotted trace). All 5-HT-ir SRa neurons dorsal to the "ventral MLF axis" are categorized as SRa-d. At this plane, only 5-HT-ir neurons within and touching the "NIn boundary" are categorized as SRa-vm—cells outside of this boundary but medial to the "lateral MLF axes" are categorized as SRa-d. Finally, all 5-HT-ir neurons ventral to the "ventral MLF axis" and lateral to the "lateral MLF axes" are categorized as SRa-vl. (d)Transverse, high magnification view of SRa-vl neurons. Caret indicates a fusiform neuron with straight bidirectional processes emerging at opposite poles of the cell. This type of cytoarchitecture is prominent in SRa-vl. (e) Transverse, high magnification view of SRa-d neurons. (f) Transverse, high magnification view SRa-vm neurons. (g) Transverse view of intermediate raphe neurons. (h) Transverse view of rostral inferior raphe (IRa) and reticular formation (RF) 5-HT cell populations. Scale Bar = 400 in a; 200 μm in b, 350 μm in c; 35 μm in d, e, f; 100 μm in g, h [Color figure can be viewed at wileyonlinelibrary.com]

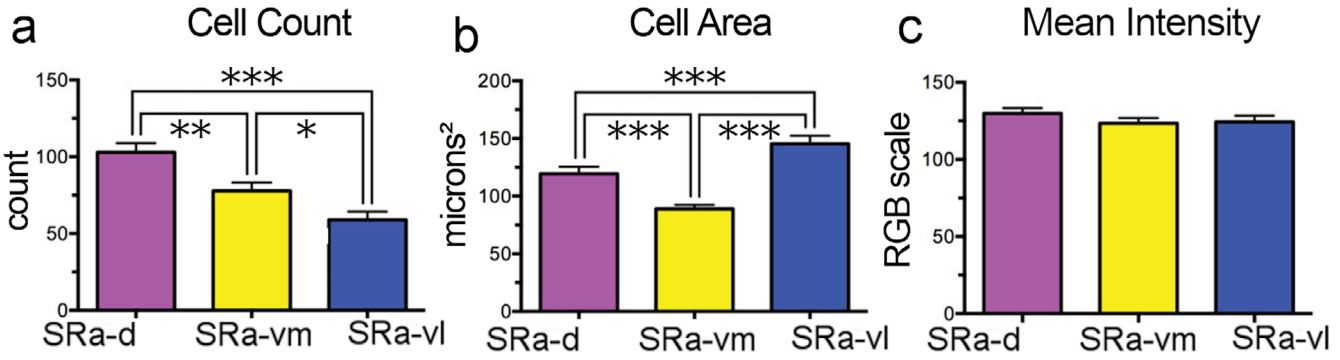

FIGURE 7 Statistical analysis of morphometric data in superior raphe (SRa) subregions (n = 16, Type I males = 7, Type II males = 9) using repeated measures ANOVA. Error bars indicate ± standard error. Asterisks indicate significant differences found between subregions after Holm–Bonferroni posthoc method. * = $p < .05$; ** = $p < .01$; *** = $p < .001$. (a) Cell number is significantly different between SRa subgroups. SRa-d = 102.94 ± 6.04, SRa-vm = 77.81 ± 5.55, SRa-vl = 58.81 ± 5.39; ($F_{(2, 30)} = 20.06$, $p < .001$). (b) Mean cross-sectional cell area is significantly different between subgroups. SRa dorsal subregion (SRa-d) = 119.62 ± 6.10, SRa ventromedial subregion (SRa-vm) = 89.10 ± 3.44, SRa ventrolateral subregion (SRa-vl) = 145.61 ± 6.98 ($F_{(2, 30)} = 50.18$, $p < .001$). (c) Mean intensity is not significantly different between SRa subgroups. SRa-d = 130.04 ± 3.42, SRa-vm = 121.69 ± 3.43, SRa-vl = 124.51 ± 4.21 ($F_{(2, 30)} = 1.766$, $p = .188$) [Color figure can be viewed at wileyonlinelibrary.com]

control nodes in the telencephalon and hypothalamus show a substantial amount of 5-HT innervation, as do sensory integration and processing areas in the thalamus, midbrain, and dorsal hindbrain. Many of the cholinergic cranial motor nerve nuclei have especially dense 5-HT signal and are dealt with in a dedicated section addressing ChAT (choline acetyltransferase) colocalization. We also studied 5-HT input in the VPG nuclei after unilateral vocal nerve backfill and this data is likewise described in its own section.

3.2.2 | Forebrain

5-HT-ir signal is strikingly low, if not absent in the olfactory bulb (Figures 3a and 4a), with only a few scattered fibers present. In the telencephalon, 5-HT-ir fiber fields exhibit marked contrasts in density between nuclei, with label ending abruptly at region boundaries. For example, the central medial zone of the dorsomedial telencephalon (Dm-cm; Figures 2e, 4a, and 10a) is markedly devoid of 5-HT signal, though its lateral periphery is bound dorsally by a dense plexus of anterior-projecting 5-HT-ir axons (Figure 10a). The most rostral region of dense 5-HT-ir terminal fields is found in the lateral zone of the rostral dorsal telencephalon (Dl; Figures 2a and 10b). Caudal to the most rostral Dl, there is a stark drop-off in Dl 5-HT-ir label (Figure 2b–d). The lateral sulcus (slat) separates the Dl from the relatively high 5-HT-ir signal in the dorsal zone of the dorsal telencephalon (Dd; Figure 2b–d). Neurons in Dl and Dc are organized in a laminar pattern and 5-HT fibers are interspersed throughout these strata (Figure 2a). The medial zone of the dorsal telencephalon (Dm) also contains high levels of 5-HT-ir fibers. 5-HT-ir in Dm is most dense medial to and along a dorsoventral strip ventral to a prominent sulcus (s; Figures 2a–d; described in Coral Reef Multiband Butterflyfish in Dewan and Tricas (2014)) and a high concentration of 5-HT-ir fibers is continuous laterally to this strip in Dd (Figure 2b). The ventral and supracommissural nucleus of the ventral telencephalon (Vv, Vs; Figures 2a,b, 3a,b, and 10e) show the highest 5-HT fiber signal in the midshipman subpallium. Prominent 5-HT-ir fiber decussations are found in the anterior commisure (ac; Figures 2b and 3b).

Periventricular 5-HT-ir fiber presence on preoptic area (POA) somata is modest, but serotonergic axons are found putatively contacting the laterally directed POA dendrites in all POA subregions: posterior parvocellular (PPp), magnocellular (PM), gigantocellular (PMg), and anterior parvocellular (PPa; Figures 2b–e, 3b, and 10i). The neuropil lateral to the caudal POA contains ascending 5-HT-ir tracts of passage entering the medial forebrain bundle (MFB; Figure 10i). Some of the densest 5-HT-ir label in the midshipman brain is located in the auditory thalamic central posterior nucleus (CP; Figures 2f, 3a, and 10f). Strong signal for 5-HT-ir fibers displaying fine putative terminals is found in the ventral tuberal hypothalamus (VT; Figures 2d and 10g,h), anterior tuberal nucleus (AT; Figure 2f), and medial and lateral divisions of nucleus preglomerulosus (PGm, PGl; Figure 2d–f). A region of intense 5-HT label is found lateral to the most rostral extent of ventral zone of the hypothalamic periventricular nucleus (Hv; Figure 2e), likely corresponding to dense collections of anterior projecting fibers of passage.

3.2.3 | Brainstem and spinal cord

The dorsal margin of the torus semicircularis (TS) contains relatively sparse, thin 5-HT-ir fibers (Figure 10j) and the TS inner core is largely devoid of 5-HT-ir. However, label abruptly becomes dense with 5-HT-ir terminals at the dorsal boundary of the deep cell layer of the TS (see Bass et al., 2000 for description of this feature) and continues ventrally to zones of very dense longitudinal 5-HT fibers near the torodiencephalic band (TD; Figures 2h,I and 10j). The paratoral tegmentum (PTT), a midbrain vocal activation site, shows dense 5-HT-ir innervation. In addition, other nodes of the midbrain vocal–acoustic complex (mVAC, see Goodson & Bass, 2002) including the nucleus of

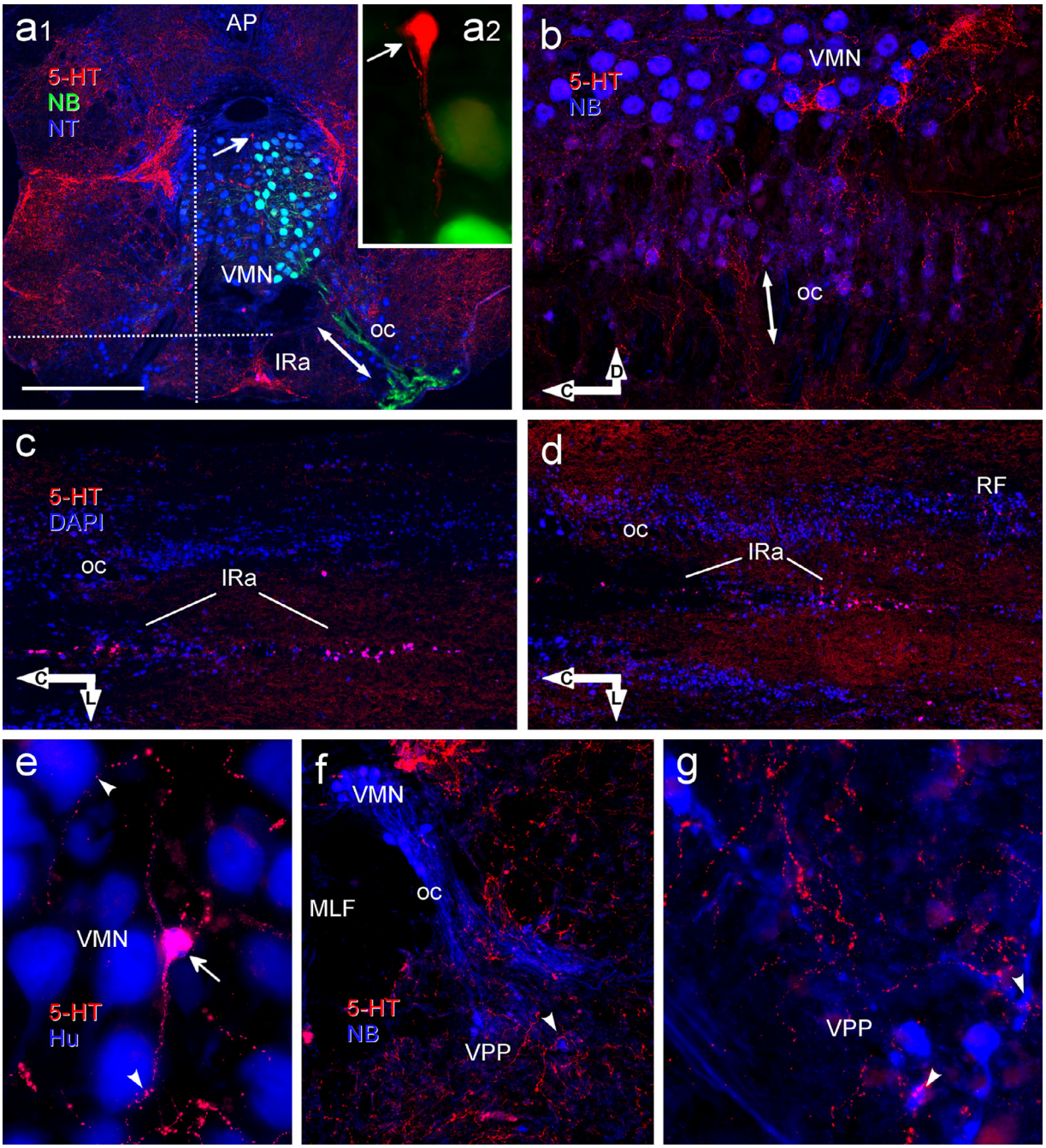

FIGURE 8 5-HT-ir (red) innervation of vocal pattern generator and proximal hindbrain 5-HT populations. (a1) Transverse brain section at the level of the hindbrain-spinal cord showing vocal motor nucleus (VMN) and caudal inferior raphe (IRa). A unilateral occipital nerve backfill utilizing Neurobiotin (NB; green) visualizes the VMN somata and axons forming the occipital nerve roots. Double-headed arrow runs parallel to the occipital nerve tract, a possible path taken by VMN-contacting efferents from the IRa. Arrow points to 5-HT-ir neuron within the boundary of the VMN. Blue is Neurotrace (NT) fluorescent Nissl. (a2) High magnification view of 5-HT-ir VMN located cells in a1 making putative contacts with backfilled VMN neuron. (b) Parasagittal plane section, with vocal neurobiotin backfill (blue) corresponding to the vertical dotted line in a. Note occipital nerve (oc) tract with adjacent 5-HT fibers entering the VMN (double-headed arrow) and motor neurons showing dense 5-HT-ir covering of putative contacts. (c) Horizontal section corresponding to the horizontal line in a. This is the rostrocaudal extent of the IRa cells. Blue is DAPI nuclear stain. (d) Horizontal section corresponding to a plane dorsal to the horizontal line in a. Note ventrolateral reticular formation 5-HT-ir cells (RF). (e) 5-HT-ir cell located in the dorsal VMN (arrow). Two processes can be seen emerging dorsoventrally from opposite sides of the cell. Both processes appear to be making putative contacts on Hu-ir VMN somata (blue). Transverse view. (f) Serotonergic innervation of vocal patterning circuit in the ventral hindbrain. Carets indicate putative 5-HT-ir contacts on vocal-backfilled cells in the vocal prepacemaker neurons (VPP; blue). Transverse view. (g) Higher magnification view of the VPP. Carets indicate 5-HT-ir puncta on backfilled somata (blue). Transverse view. Scale bar = 500 μm in a1; 50 μm in a2; 200 μm in b; 500 μm in c, d; 50 μm in e; 200 μm in f; 100 μm in g [Color figure can be viewed at wileyonlinelibrary.com]

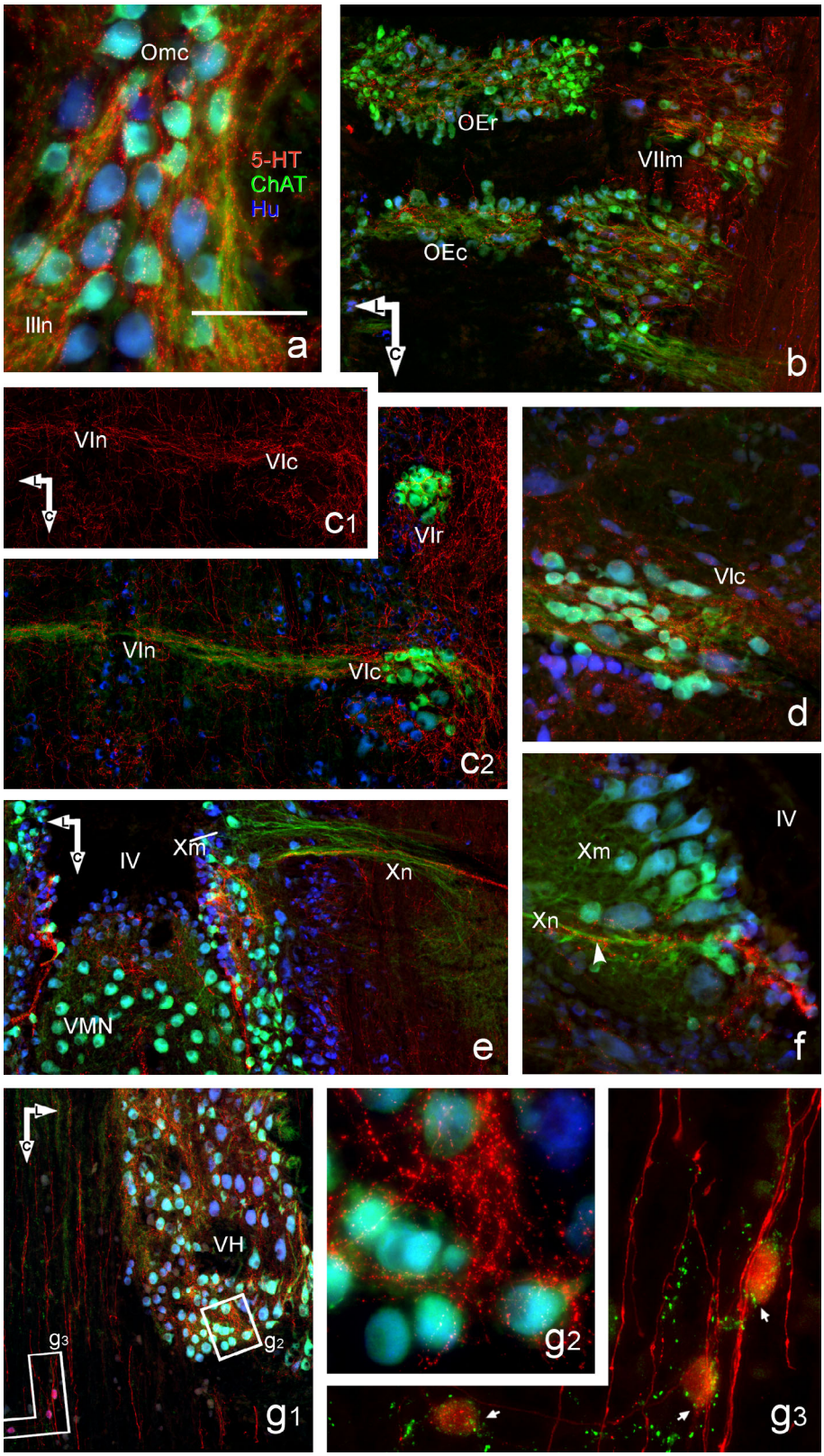

FIGURE 9 5-HT-ir (red) innervation of cholinergic cranial motor nuclei labeled by choline acetyltransferase (ChAT; green). Arrow indicates caudal (C) and lateral (L) directions in horizontal sections. (a) Transverse view of robust 5-HT-ir fibers in the oculomotor complex (Omc), showing putative synapses on both somata and processes in the vicinity of the oculomotor nerve tract (IIIn). (b) Horizontal view of rostral and caudal octaval auditory efferent nucleus (OE-r, OE-c) and facial motor nucleus (VIIm) showing dense 5-HT-ir fibers. Note longitudinal 5-HT tracts on the right. (c1-2) Horizontal view of rostral and caudal abducens motor nucleus (VIr, VIc) showing robust 5-HT-ir fiber label. (c1) 5-HT alone. Note medially projecting bilateral decussation following the VIn ascending tracts. (c2) Same view showing ChAT-ir overlap. 5-HT-ir decussation overlap with VIn axons is evident. (d) Dense 5-HT-ir putative contacts on VIc somata. Transverse view. (e) Horizontal view of hindbrain-spinal cord boundary. Note 5-HT-ir fibers in the VMN, vagal motor nucleus (Xm), and longitudinal serotonergic tracts at the VMN periphery. (f) Xm in transverse view. Note the 5-HT-ir fibers contiguous with the axonal tracts of the vagus nerve (Xn). (g1) Horizontal view of the spinal cord. Thick medial longitudinal 5-HT-ir fibers can be seen on the left of the picture. The ventral horn (VH) contains substantial 5-HT-ir fiber label. (g2) Inset from g1 of VH cholinergic neurons covered by a dense 5-HT-ir terminal field. (g3) Inset from g1 of 5-HT spinal neurons showing cholinergic putative synapses (arrowheads). Scale bar = 60 μm in a; 200 μm in b; 267 μm in c1; 200 μm in c2; 100 μm in d; 500 μm in e; 100 in f; 200 μm in g1; 35 μm in g2, g3 [Color figure can be viewed at wileyonlinelibrary.com]

the lateral lemniscus (nll), PAG, and paralemniscal midbrain tegmentum (PL) receive substantial 5-HT input (Figures 2i,j, 10k).

5-HT-ir fibers are found in the midbrain tectum (TeM, Figures 2g-k,3a,4a,5b, and 10l) with dense transverse bands in stratum fibrosum et griseum superficiale (sfgs), stratum griseum centrale (sgc), and more diffuse axons in stratum album centrale (sac; Figure 10l). Sections labeled with both 5-HT-ir and ChAT-ir, show relative laminar segregation of serotonergic signal compared with transverse cholinergic

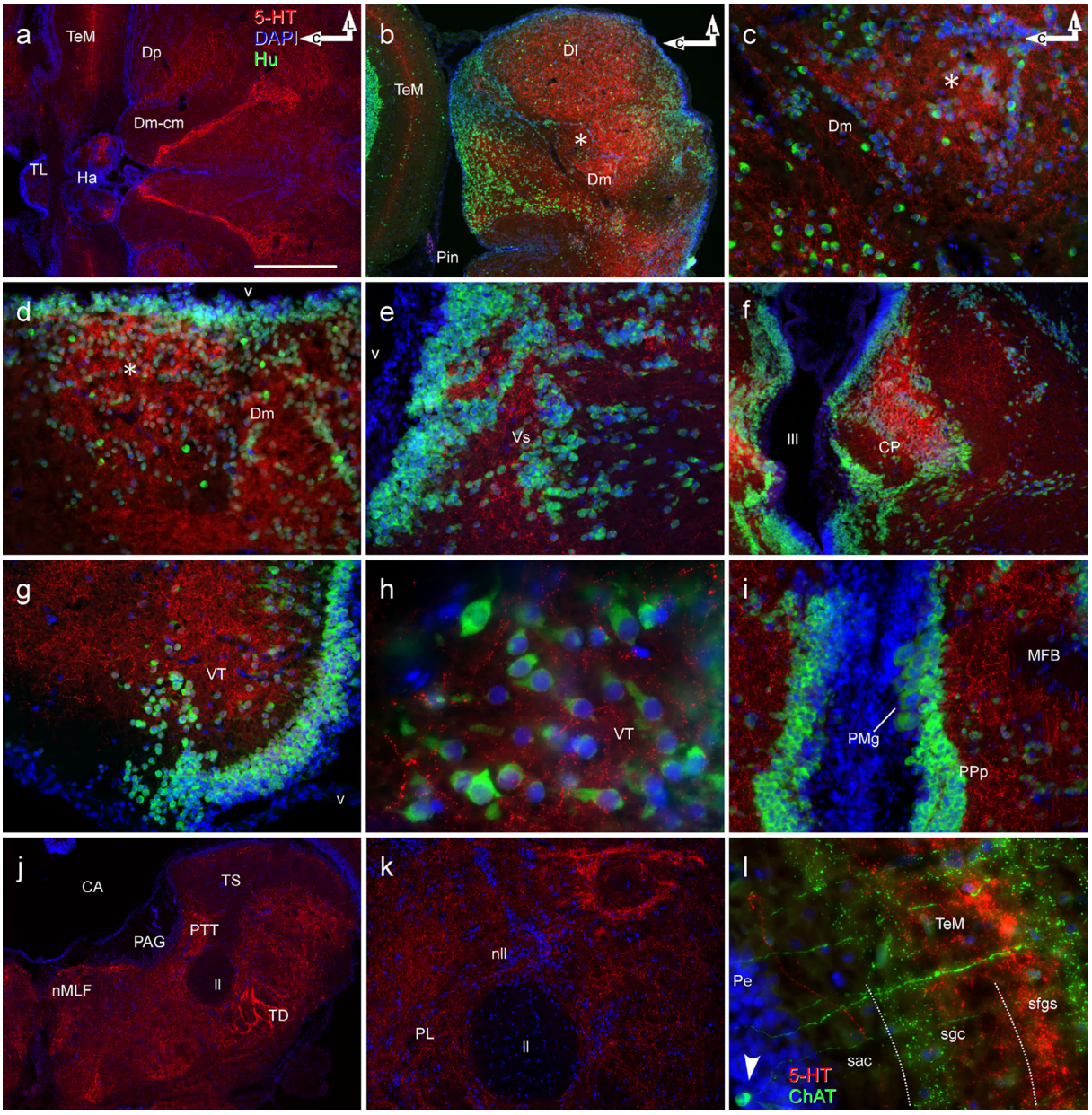

FIGURE 10 Forebrain and midbrain 5-HT-ir (red) fibers. Arrows indicate caudal (C) and lateral (L) directions in horizontal sections. (a) Horizontal view of the dorsal forebrain and dorsal midbrain with robust ascending 5-HT-ir fiber tract present throughout the dorsal telencephalon located just outside the dorsal boundary of the central medial zone of the dorsomedial telencephalon (Dm-cm). The Dm-cm itself is conspicuously devoid of 5-HT-ir. (b) Horizontal view of dorsomedial telencephalon (Dm) and rostral midbrain. Asterisk indicates area of high 5-HT-ir fiber density in Dm. (c) High magnification horizontal view of Dm as shown in previous figure (b). Asterisk corresponds to relative location as in figure b. (d) Transverse view of the dorsal telencephalon. Note the especially fine fiber diameter of 5-HT-ir points in this region. Asterisk corresponds to relative location as in figures b, c. (e) Transverse view of the ventral telencephalon with emphasis on substantial 5-HT fiber presence in the supracommissural nucleus of ventral telencephalon (Vs). (f) Dorsal thalamus, transverse view centered on the auditory thalamic central posterior nucleus (CP). This region contains dense 5-HT-ir terminal fields resembling the fine 5-HT fiber appearance in Dm (c, d). (g) Rostral hypothalamus, including the ventral tuberal hypothalamus (VT). Transverse view. (h) High magnification view of VT cells in previous figure (g) with putative 5-HT-ir terminals on VT cells. Transverse view. (i) Caudal preoptic area (POA) in transverse view. Putative 5-HT-ir terminals at contact sites in proximity of POA dendrites. (j) Low magnification transverse view of the midbrain. High levels of 5-HT-ir are present in vocal-auditory integration areas with especially dense signal found in the PTT. The central core of the torus semicircularis (TS) is largely devoid of 5-HT-ir although some fibers are present in the dorsal TS near the cerebral aqueduct (CA). (k) Higher magnification of subset of vocal- motor areas of the midbrain: Paralemniscal nucleus (PL), nucleus of lateral lemniscus (nll). Transverse view. (l) High magnification transverse view of the midbrain tectum (TeM). Dashed lines indicate tectum strata: stratum album centrale (sac), stratum fibrosum et griseum superficiale (sfgs), stratum griseum centrale (sgc), and periventricular cell layer of the midbrain tectum (Pe). The caret indicates a cholinergic neuron with transverse process traversing several strata. Note the nonoverlap of 5-HT-ir and ChAT-ir fibers and numerous ChAT-ir fibers perpendicular to the 5-HT-ir band. Scale bar = 500 μm in a, b; 100 μm in c, d, e; 200 μm in f; 100 μm in g; 50 μm in h; 100 μm in i; 500 μm in j; 200 μm in k; 50 μm in i [Color figure can be viewed at wileyonlinelibrary.com]

fibers. Both 5-HT-ir projection axons and terminal fields are abundant in tegmental nuclei, with staining heavy in the nucleus of the medial longitudinal fasciculus (nMLF; Figure 10j).

The auditory and mechanoreceptive recipient areas of the midshipman hindbrain robustly express 5-HT-ir. The primary lateral line processing nucleus medialis (MED; Figures 2l–o and 4a), found ventral to the cerebellar crest and extending through most of the dorsal medulla, contains especially high 5-HT-ir fiber density. The caudal and rostral divisions of the octavalateralis efferent nucleus are both densely innervated by 5-HT fibers (OE-c, OE-r; Figure 9b) as are the dorsolateral and dorsomedial divisions of the auditory dorsal descending octaval nucleus (dl and dm; Figure 2n,o).

3.2.4 | Vocal pattern generator

The midshipman VPG is a motor efferent circuit comprised of three nuclei: VPP neurons, vocal pacemaker neurons (VPN), and VMN, the last being a greatly expanded homolog to the hypoglossal (XII) cranial motor nucleus (Bass, Gilland, & Baker, 2008). Consistent with previous studies, occipital nerve backfills were successful in delineating all three VPG regions, which are thought to be connected through gap junctions (Bass et al., 1994; Chagnaud, Zee, Baker, & Bass, 2012). It was not expected that the chemical synapses found in the serotonergic system would facilitate transneuronal labeling, although 5-HT-ir process presence on backfilled neuronal elements suggests 5-HT synaptic input.

Vocal motor neuron somata and dendrites appear to receive contacts from 5-HT-ir varicosities projecting from serotonergic interneurons within the nucleus itself (Figures 4b and 8a,e). The extensive distribution of 5-HT fibers in the whole VMN strongly suggest that additional sources of 5-HT are found outside of the nucleus, perhaps originating in the ventromedial inferior raphe neurons found near the spinal cord/hindbrain boundary ventral to the VMN (Figures 4b and 8c,d). Several routes by which IRa fibers enter the VMN seem most likely; 5-HT axons may course dorsally between the MLF and either enter the VMN at its ventral base or fan out laterally entering in the occipital tract (double-headed arrows in Figure 8a1,b). 5-HT fibers may also enter the VMN from rostral medullar IRa neurons in the ventral medulla (Figure 4b1,e). The rostral VMN seems to exhibit greater 5-HT-ir fiber density compared with more caudal VMN, and fibers may also enter the VMN at its rostral boundary near vagal lobes (Figure 9e). 5-HT-ir puncta are also found on VPP cell bodies (carets in Figures 8f,g), suggesting multiple anatomical levels for serotonin's neuromodulatory action on VPG output.

Fibers showing strong 5-HT-ir are found dorsolateral to the VMN and ventral to the AP in extensive and dense laterally fanning tracts (Figures 2p,q, 4b and 8a1) coregional with catecholaminergic tracts (see Forlano et al. (2014) and neuropeptidergic fibers (see Goodson, Evans, and Bass (2003). We did not observe any 5-HT-ir fibers within cranial nerves or sensory ganglia, suggesting that these serotonergic hindbrain tracts ultimately descend down throughout the dorsal spinal cord.

3.2.5 | Cholinergic motor nuclei

The dense terminal fields formed by 5-HT-ir in midshipman cranial motor nuclei deserve special mention since these form some of the heaviest label of serotonergic innervation we found. While all somatomotor nuclei exhibit strong 5-HT-ir innervation, the combined factors of the large size of motor neuron somata and the very fine caliber of serotonergic axons can result in a sparser appearance at lower magnifications, notably in the VMN.

The midshipman oculomotor complex (OMc; see Brantley & Bass, 1988) contains the expansive, medial mesencephalic nucleus III and the dorsolateral and relatively smaller rhomboncephalic nucleus IV (Gilland, Straka, Wong, Baker, & Zottoli, 2014). Ascending serotonergic tracts appear to traverse the oculomotor nerve efferent tract (IIIn; Figure 9a) en route to the forebrain and a certain proportion of the 5-HT-ir processes in this area are probably fibers of passage. However, the majority of 5-HT-ir fibers in OMc are highly varicose and exhibit axonal swelling abutting ChAT-ir somata and dendrites, suggesting the presence of neuromodulatory 5-HT terminals and release sites. The rostral and caudal divisions of the abducens nucleus (VIr, VIc; Figure 9c,d), another somatomotor extraocular nucleus, contains dense 5-HT-ir fiber label on ChAT-ir somata and dendrites. 5-HT-ir processes follow both VI ascending tract decussations toward the midline, likely following descending spinal column tracts (VIn; Figure 9c).

The octavalateralis efferent nucleus (rostral division- OEr, caudal division- OEc) and facial motor nucleus (VIIm) show strong 5-HT-ir label with dense punctate fibers surrounding somata and dendrites (Figure 9b). The vagal motor nucleus (Xm; Figure 9e,f) shows scattered 5-HT-ir label on somata and along the vagal motor tract (Xn). As mentioned, the VMN also contains 5-HT-ir fibers throughout (Figure 9e).

The spinal motor region in the ventral horn (VH; Figure 9g1) appears to exhibit reciprocal interaction between the cholinergic and serotonergic systems. Very fine putative terminal densities are found on ventrolateral ChAT-ir neurons (Figure 9g2). Ventromedial, longitudinally bipolar 5-HT-ir spinal neurons display close putative ChAT-ir boutons on their somata and proximal processes (arrows in Figure 9g3). The differential fiber thickness found in the serotonergic system is evident throughout the brain, but is prominent in this region. Whereas fields of very fine, highly punctate fibers surround the aforementioned cholinergic spinal neurons, the more medial, highly longitudinal processes emerging from spinally located 5-HT-ir somata are relatively thick and smooth, with occasional swellings potentially indicating en passant release sites.

4 | DISCUSSION

Our investigation of serotonin immunoreactivity in the midshipman brain can broadly be grouped into two themes: (a) comprehensive and comparative neuroanatomical analysis of the 5-HT system in a teleost fish, including a quantitative analysis of the size and number of brainstem (superior raphe) 5-HT-ir populations. (b) The localization of

5-HT-ir innervation of vocal and auditory circuitry and potential functional implications in the midshipman fish model system. Mapping of the serotonergic system, combined with the extensive knowledge of the functional neuroanatomy of this species, provides insight into potential roles for this neuromodulator and sets a foundation for studying this system through additional techniques and with an emphasis on future insights regarding comparisons between adult midshipman reproductive phenotypes as well as other vocal vertebrate species.

4.1 | Comparative 5-HT-ir distribution

Numerous studies have used antibodies against serotonin to study its CNS distribution in various fish species (Bolliet & Ali, 1992; Bolliet, Perreault, & Ali, 1994; Corio, Peute, & Steinbusch, 1991; Ekström, Östholm, & Ebbesson, 1992; Ekström & Van Veen, 1984; Gotow et al., 1990; Kah & Chambolle, 1983; Kaslin & Panula, 2001; Khan & Thomas, 1993; Lillesaar, Stigloher, Tannhäuser, Wullimann, & Bally-Cuif, 2009; Lorenzi & Grober, 2012; Meek & Joosten, 1989; Oliveri, Candiani, Parodi, Bertini, & Pestarino, 2005; Rodríguez-Gómez, Rendón-Unceta, Sarasquete, & Muñoz-Cueto, 2000). Our cell and fiber distribution results are largely in agreement with those of other teleost species, including those in the widely used zebrafish (*Danio rerio*) teleost model (Lillesaar, 2011). However, we have sought in the present study to provide the most detailed neuroanatomical atlas of the distribution of 5-HT-ir in a teleost to date. Our analysis has also yielded a number of potentially derived features of the midshipman 5-HT system, namely an especially extensive ventromedial medullar 5-HT population and a VMN 5-HT population which may be related to specialized brain areas involved in vocal behavior in this species.

The anatomical subdivision scheme of the serotonergic raphe in mammals, proposed in Dahlstroem & Fuxe (1964), has been adopted in teleost research (Bolliet & Ali, 1992; Ekström & Van Veen, 1984; Kaslin & Panula, 2001) owing to the exceptional degree of cross-taxa conservation of the location of brainstem 5-HT cells. The vertebrate raphe as a whole contains both serotonergic and nonserotonergic cells (Gaspar & Lillesaar, 2012). However, genetic studies have revealed that the serotonergic raphe expresses transcription factors (notably ETS-domain factor Pet-1) not found in non-5-HT cells and that are necessary for the development of the brainstem 5-HT system (Cheng et al., 2007). Our anatomical description and general nomenclature is thus informed by the substantial body of comparative research on serotonin. However, we have strived for the most parsimonious naming scheme that can be justified by the anatomical evidence, and have tried to avoid a purely a priori designation approach based on potentially superficial comparative resemblances.

The raphe of fishes and other vertebrates is usually divided into superior (SRa) and inferior regions (IRa) (Nieuwenhuys, 2011), which send ascending and descending projections, respectively (Lillesaar et al., 2009). We identified a population of 5-HT-ir cells just rostral to the abducens motor nucleus that is longitudinally discontinuous from either SRa or IRa and have designated this group the intermediate raphe (ItRa) due to its distinct location and morphological features compared with the other raphe groups (Figures 3b and 6g). Neurons in ItRa are typically found in bilateral clusters ventrolateral to the MLF interspersed between large reticular neurons and appear to send descending projections. In sockeye salmon fry, neurons matching this description were tentatively named raphe magnus, corresponding to group B3 in the inferior raphe (Ekström & Ebbesson, 1989). The mammalian raphe magnus is an extensive population of typically medial neurons found at the level of, and caudal to, the facial motor nucleus (Alonso et al., 2013; Hornung, 2003). Although a rostral and lateral migration, as well as fewer cells within the raphe magnus in fishes relative to mammals is a possibility, we suggest that the ItRa is not homologous to the raphe magnus. The average cell area of ItRa neurons is significantly smaller than that in IRa, but not SRa. One possibility is that the ItRa corresponds to group B5, the pontine raphe (Alonso et al., 2013). This population is not well understood and further research in midshipman or other species may provide needed comparative and functional insight. Based on neuroanatomical comparisons (Hermann et al., 1997), we propose the midshipman rostral IRa appears to be a more likely homolog to raphe magnus, while the caudal IRa is likely homologous to raphe pallidus and raphe obscurus.

Here we mapped the neuroanatomy of serotonin in a batrachoidid fish. In the closely related socially vocal batrachoidid Gulf toadfish (*Opsanus beta*) the (inhibitory) 5-HT1A (Medeiros, Mager, Grosell, & McDonald, 2010) and (excitatory) 5-HT2A (Mager, Medeiros, Lange, & McDonald, 2012) receptors have been cloned and quantified through quantitative real-time PCR. In the case of both receptors, relative transcript levels were lowest in the cerebellum and olfactory bulb, matching our pattern of 5-HT-ir presence. Otherwise high levels in the forebrain, midbrain, and hindbrain suggests that these receptors mediate the action of serotonin at these levels of the toadfish brain and it is expected that midshipman synaptic modulation operates in part through these two G-protein-coupled receptors. Since substantial levels of 5-HT1A and 5-HT2A are reported in the swim bladder of toadfish (5-HT1A was also present in the vocal muscle but was not assayed for 5-HT2A), we surveyed both swim bladder and vocal muscle from midshipman but did not observe any above-background 5-HT-ir in either tissue (data not shown), suggesting input from circulating 5-HT. While we cannot rule out isolated areas of 5-HT-ir missed in our histological survey, it is an intriguing possibility that 5-HT may modulate vocal output at the level of the sound-generating organs.

4.2 | 5-HT-ir innervation of vocal circuitry

The midshipman VMN is the homolog of the tetrapod hypoglossal nucleus (XII) which is involved in innervating the tongue, syrinx, or pectoral fin components of sonic communication in mammals and bullfrogs, birds, and channel catfish, respectively (2016). The VMN comprises the final neural output node underlying social vocalizations produced by midshipman and is hypertrophied in the "singing" morphotype "I" males (Feng & Bass, 2017). We identified 5-HT-ir cells

within the boundaries of the VMN that form putative contacts on vocal motor neurons. Synaptic input on VMN somata and dendrites are associated with both excitatory and inhibitory modulation and have been suggested as indicative of 5-HT synapses (identified via electron microscopy in Bass & Marchaterre, 1989). The neuroanatomical identity of VMN 5-HT cells is unclear since, to our knowledge, there is no documentation of serotonergic neurons within the hypoglossal nucleus in other species. One possibility is that these cells are continuous with neurons in the caudal IRa, which are ventral to the VMN and likely supply serotonin to vocal motor neurons, as well. Since the midshipman VMN is so large, a consequence may be the incidental development of some medullar 5-HT cells within its boundaries. However, VMN 5-HT-ir cells are interspersed throughout the VMN and often found near the fourth ventricle more dorsal than cells in the IRa. VMN 5-HT-ir cells also appear smaller in area, though this has not been quantified. Furthermore, since VMN 5-HT-ir cells display local putative innervation of vocal motor neurons, a role related to vocal output may suggest functional specialization of these 5-HT neurons. Thus, a condition in midshipman of a distinct, if relatively small, population of derived VMN 5-HT neurons corresponding to behaviorally adapted vocal neuroanatomy is a fascinating possibility.

Neuronal and fiber label for 5-HT in the midshipman VPG resembles that found in recent immunohistochemical research in Gulf toadfish (Rosner et al., 2018). The Gulf toadfish VMN receives serotonergic processes, forming putative contacts, from cells situated ventral to it in the IRa, as well as 5-HT-ir neurons found within the VMN itself. VPP and VPN somata and dendrites likewise show 5-HT-ir signal, in line with our findings.

Previous research utilizing neuronal tracing techniques in batrachoidids has outlined reciprocal connectivity between vocal activation regions in the forebrain and midbrain as well as auditory input into those areas (Goodson & Bass, 2002; Kittelberger & Bass, 2012). Components of sites subject to vocal elicitation are grouped into the forebrain vocal-acoustic complex (fVAC), comprised of the anterior (PPa), and posterior (PPp) parvocellular preoptic nuclei, and the anterior (AT) and ventral tuberal (VT) nuclei (see Figure 1a). Midbrain sites exhibiting said physiological activity are grouped into the midbrain vocal-acoustic complex (mVAC), comprised of nuclei in the dorsal tegmentum, namely, the PAG, PTT, and paralemnsical tegmentum (PL), nucleus of the lateral lemniscus (nll), isthmal nucleus (Is), and isthmal paraventricular cell group (IP). As evident in the Figure 2, all fVAC sites contain 5-HT-ir fibers and putative serotonergic innervation is especially heavy in PPa and VT. All mVAC sites contain dense 5-HT-ir terminal fields.

In the African clawed frog (*Xenopus laevis*) sex typical calls can be initiated via application of 5-HT or pharmacological facilitation of endogonous 5-HT in an *in vitro* brain preparation (Rhodes et al., 2007) and this action is mediated through 5-HT2C receptors in or upstream of the VPG (Yu & Yamaguchi, 2009; Yu & Yamaguchi, 2010). The function of 5-HT in midshipman vocalization can be hypothesized to act in a similar manner and the presence of 5-HT-ir varicosities in the midshipman VPG supports such a role.

4.3 | 5-HT-ir innervation of auditory nuclei

The auditory thalamus (CP) shows the most dense 5-HT-ir terminals in all major auditory nuclei, and likely contains some of the densest innervation in the CNS. The midshipman CP receives auditory information from the TS and, as in goldfish, may function in the processing of wideband spectra characteristic of natural sound sources (Lu & Fay, 1995). Expression of the immediate early gene product cFos is robust in Type I males exposed to the advertisement call (hum) of other males versus ambient noise, suggesting a key role in differentiating conspecific auditory cues in the environment (Petersen et al., 2013). In support of this, a recent study in female midshipman demonstrated greatest cFos activation in CP after exposure to male hums compared to heterspecific vocalizations or ambient noise (Mohr et al., 2018). The highly robust 5-HT-ir found in CP suggests that serotonin may play a role in modulating the contextual salience and cognitive discrimination of social communication. Such modulation may function directly through serotonergic input onto CP neurons or through GABAergic interneurons in the CP as GABA-ir is highly expressed in the midshipman CP (Timothy & Forlano, unpublished observations). An auditory relay upstream and reciprocally connected with CP is composed of the rostral dorsomedial telencephalon (Dm) and supracommissural nucleus of the ventral telencephalon (Vs) (Goodson & Bass, 2002). All three regions show dense putative innervation by fine 5-HT-ir fibers.

Our finding of 5-HT-ir fibers in the hindbrain descending octaval recipient nucleus may indicate serotonergic modulation of audition in second-order systems as well in the midbrain and forebrain. In bats, 5-HT may enhance the activity of populations of neurons in the auditory midbrain in response to conspecific vocalizations (Hurley & Pollak, 2005). 5-HT response in the inferior colliculus of mice following social auditory stimuli shows specificity relative to behavioral or environmental context (Hurley & Sullivan, 2012). Release of 5-HT from the mouse dorsal raphe may in turn be regulated, in a context-dependent manner, by arginine vasopressin input from hypothalamic cells (Petersen & Hurley, 2017). However, whereas the rodent inferior colliculus and cochlea are highly innervated by 5-HT, the level of 5-HT-ir fibers in the midshipman auditory torus is relatively low and 5-HT is absent in the saccule, suggesting caution in a comparison to mammalian serotonergic auditory modulation. Perhaps 5-HT auditory modulation in fish may act more via hindbrain and forebrain auditory centers. However, the robust 5-HT-ir in OE may be a way of indirectly modulating peripheral auditory function through contacts on cholinergic saccular efferents. We conclude that these areas, which are integral to social communication output and integration, receive direct and substantial 5-HT input thus strongly suggesting serotonergic modulation of these behaviors.

4.4 | 5-HT-ir innervation of other neuromodulator systems

Serotonin interacts with virtually every neuromodulation biochemical and elaborating on system specific details is beyond the scope of this discussion. However, interactions with dopamine and acetylcholine are

mentioned due to the detection of 5-HT-ir fibers on somata and dendrites producing these neurochemicals as identified through multiple-antibody immunohistofluorescence methods. We performed co-labeling with tyrosine hydroxylase (TH), the rate limiting enzyme for catcholamine synthesis and choline acetyltransferase (ChAT), which is necessary for acetylcholine synthesis. Dopaminergic (DA) neurons in the TPp show putative contacts from varicose 5-HT-ir fibers likely originating in csf-contacting serotonergic cells in the hypothalamus. Notably, TPp neurons project to both the midshipman inner ear and the octavalateralis efferent nucleus (Forlano et al., 2014; Perelmuter & Forlano, 2017) and this evidence presents the possibility of auditory modulation through a chemoreceptive 5-HT-to-DA pathway.

The presence of dense 5-HT-ir varicosities on somata and dendrites of cholinergic cranial motor nuclei is notable in the high degree of label, presenting strong anatomical evidence for direct 5-HT modulation of craniomotor efferents. Indeed, serotonergic synapses are found on somatomotor neurons in mammals (May, Baker, Vidal, Spencer, & Baker, 1987). However, no 5-HT-ir fibers were observed in any cranial nerve. Studies utilizing single unit recording methods in the inferior raphe of behaving mammals have lead a compelling hypothesis for a fundamental role of 5-HT in the facilitation of motor output with concurrent sensory inhibition (Jacobs & Fornal, 1993; Miles & Sillar, 2011). Serotonin in mammals appears to excite motor neurons by enhancing their response, via 5-HT2 receptors, to ionotropic neurotransmitters (Jacobs & Fornal, 1993).

Serotonin appears to have a central role in fatigue. Evidence suggests that serotonergic firing in the feline inferior raphe facilitates tonic motor output and downregulates output in response to fatigue-related motor deficits associated with prolonged locomotor output (Jacobs & Fornal, 2010). Type I male midshipman produce sustained, metabolically demanding, courtship calls through the rhythmic activation of vocal muscles, and do so under conditions of limited nutritive opportunities (Forlano, Ghahramani et al., 2015; Forlano, Sisneros, et al., 2015; Sisneros, Forlano, Knapp, & Bass, 2004). In rats, retrograde tracing has indicated that the hypoglossal nucleus receives 5-HT input from all nuclei in the inferior raphe, though not from dorsal raphe (Li, Takada, & Mizuno, 1993). As mentioned, the midshipman IRa appears to be especially robust and the VMN (hypoglossal homolog) receives substantial 5-HT-ir fiber input. Preliminary analysis of 5-HT-ir fibers in the VMN suggests significantly higher density and intensity in Type I versus Type II morphotypes (Timothy, Ghahramani, Gorbonosov, Ferrari, & Forlano, 2014). Thus, the hypothesis that 5-HT tone is crucial to initiating motor output as well as regulating fatigue in a reproductively adaptive context is novel and compelling. Interestingly, comparative analyses of catecholaminergic innervation of VMN has shown significantly higher levels in Type II males (Ghahramani et al., 2015), suggesting an inverse relationship between different monoamines in vocal behavior.

4.5 | Quantitative comparison of superior raphe cells

In creating our descriptive atlas, preliminary observation of SRa cell distribution roughly followed the dorsal raphe/median raphe pattern outlined in canonical teleost 5-HT atlases (e.g., Ekström and Van Veen (1984); Batten, Berry, Maqbool, Moons, and Vandesande (1993). However, closer examination of the midshipman raphe revealed distinct distributional and morphological characteristics that were more nuanced than anticipated, specifically the seeming contrasts in cell size between the ventral population and the lateral population. In addition, the dorsal raphe/median raphe scheme did not account for the ventrolateral 5-HT-ir neurons we found and previously identified as part of the superior reticular formation in some fishes (e.g., Rodríguez-Gómez et al., 2000). This seeming incongruity between our observations of the neuroanatomy of the midshipman SRa and the subregion scheme adopted in teleost literature is almost certainly not due to a derived state of the midshipman SRa but rather the likely result of prior research interpreting the teleostean SRa as being directly divisible within a simplified mammalian paradigm.

Importantly, this issue goes beyond one of only descriptive anatomy. In reviewing prior studies on the superior raphe of fishes in which quantitative methodologies were utilized to test a variety of subregionial or axial distribution-based functional hypotheses in behavioral contexts, we found that there is often minimal anatomical landmark specification (especially in the rostrocaudal axis) establishing raphe subdivision demarcations that denote areas for comparative analysis. Consequently, there is the danger of these studies drawing conclusions of differential raphe subregion function based on relatively arbitrary and inexact *a priori* extrapolation from basic mammalian neuroanatomical correlates passed down through the teleost literature. Our goal was thus to identify subregions of the midshipman raphe utilizing a scheme of unambiguous placement relative to universal landmarks in the brainstem of all teleosts. The SRa-d, SRa-vm, and SRa-vl boundaries were designated based on this consideration and because these regions roughly correspond to the dorsal raphe, median raphe/interpeduncular nucleus, and superior reticular formation partitions, respectively, which are identified in the majority of canonical teleost 5-HT literature.

Morphometric analysis of cell counts and measurements showed significant heterogeneity between all three subregions in both cell counts and cross-sectional area (Figure 7). 5-HT-ir cells were most numerous in SRa-d followed by SRa-vm, with the fewest cells found in SRa-vl. This robust directional difference in neuronal density between subregions supports both the predictive value and anatomical validity of the proposed boundaries. The considerable contrast in average 5-HT-ir cell area between subregions, with SRa-vl somata having the largest cross-sectional area, followed in size by SRa-d, and then SRa-vm supports our hypothesis of substantial and biologically significant morphological heterogeneity between subregions, suggesting phenotypic and functional differences between the proposed cell groups. Finally, the very close agreement in average intensity between groups can be interpreted as supporting the validity of our cross-sectional area results, since a sizable difference in 5-HT label brightness between subregions could potentially indicate a methodological confound related to inconsistent observer tracing of cells, variance in immunohistochemical binding, or issues related to the plane in which cells are situated.

We are cautious of assigning comparative identities to the three midshipman SRa subregions described but a tentative interpretation follows. The SRa-vl can be interpreted to correspond and encompass the supralemniscal nucleus (B9) and pontomesencephalic reticular formation (Vertes & Crane, 1997). The most ventrolateral population of SRa-vl in zebrafish and stickleback has also been noted as a separate group based on its contrasting location relative to other SRa populations and its resemblance to the mammalian B9 (Ekström, 1994; Lillesaar et al., 2009). However, transgenic facilitated tracing from the zebrafish ventrolateral population showed a projection pattern terminating exclusively in the preglomerular complex, which contrasts with the more widespread targets of the mammalian B9 (Lillesaar et al., 2009).

Speculating on comparative anatomical homologs of SRa-d and SRa-vm is more difficult than SRa-vl. In mammals and birds, the dorsal raphe fans out laterally at the level of the locus coeruleus (Parent, Wallman, Gagnon, & Parent, 2011) and is relatively easily separable from the median raphe. This pattern is absent in midshipman, with most SRa cells outside of SRa-vl occupying a medial location, though a portion of SRa-d cells are lateralized (Figure 6b). The most straightforward approach would be to associate SRa-d with dorsal raphe (B6, B7) and SRa-vm with central/median raphe (B5, B8), though this overlap is considerably inexact.

It may be that the looking for B5-B9 homologs in fish based on direct anatomical juxtaposition is misguided and teleostean raphe functional heterogeneity should be approached with fresh expectations. Elegant work in zebrafish does suggest functional projection specialization along a SRa-d/SRa-vm axis. Dorsoventral position and neuronal size of SRa neurons is significantly associated with differing forebrain targets: ventral SRa cells and those with larger cell bodies tend to project to the hypothalamus compared to dorsal and smaller SRa cells that target the telencephalon and olfactory bulb (Lillesaar et al., 2009). The midshipman model provides a well-studied evolutionary and physiological framework with which to test hypotheses regarding conservation of raphe subregion identity and function.

5 | CONCLUSION

The plainfin midshipman is an excellent model for studying the contrasts and similarities of evolutionarily conserved chemical neuroanatomy, especially in relation to intraspecific social communication. The 5-HT system in midshipman is largely conserved, though possibly exhibiting derived features in hindbrain populations related to vocal output. Moreover, our detailed analysis of 5-HT-ir neurons in the isthmus and pons presents a rigorous and comprehensive interpretation of teleostean comparative anatomy. The presence of dense 5-HT fibers exhibiting cytomorphological features indicative of 5-HT release and modulation in previously documented vocal and auditory processing nodes strongly suggests a role in higher order sensorimotor processing and behavioral integration in our model. We believe our atlas of brain serotonin provides insights as to the comparative anatomy of this neurochemical and establishes a robust, high resolution foundation from which to elucidate detailed functional and behavioral relevance that can be extended across vertebrate taxa.

ACKNOWLEDGMENTS

We thank the University of California, Davis Bodega Marine Lab, Sisneros Lab, and Midge Marchaterre for logistical support, Zachary Ghahramani for tissue preparation assistance and valuable statistical methodology insight, Michelle Gorbonosov and Alena Chernenko for performing image analysis and support by National Science Foundation IOS 1456743 (P.M.F.)

CONFLICT OF INTEREST

The authors declare no known or potential conflicts of interest.

DATA AVAILABILITY STATEMENT

The data that support the findings of this study are available from the corresponding author upon reasonable request.

ORCID

Miky Timothy https://orcid.org/0000-0002-4266-2403
Paul M. Forlano https://orcid.org/0000-0003-4258-5708

REFERENCES

Adrio, F., Anadón, R., & Rodríguez-Moldes, I. (2000). Distribution of choline acetyltransferase (ChAT) immunoreactivity in the central nervous system of a chondrostean, the siberian sturgeon (*Acipenser baeri*). *The Journal of Comparative Neurology*, *426*(4), 602–621. https://doi.org/10.1002/1096-9861(20001030)426:4

Adrio, F., Anadón, R., & Rodríguez-Moldes, I. (2002). Distribution of tyrosine hydroxylase (TH) and dopamine β-hydroxylase (DBH) immunoreactivity in the central nervous system of two chondrostean fishes (*Acipenser baeri* and *Huso huso*). *The Journal of Comparative Neurology*, *448*(3), 280–297. https://doi.org/10.1002/cne.10256

Albersheim-Carter, J., Blubaum, A., Ballagh, I. H., Missaghi, K., Siuda, E. R., McMurray, G., … Gray, P. A. (2016). Testing the evolutionary conservation of vocal motoneurons in vertebrates. *Respiratory Physiology & Neurobiology*, *224*, 2–10. http://dx.doi.org/10.1016/j.resp.2015.06.010

Alonso, A., Merchán, P., Sandoval, J. E., Sánchez-Arrones, L., Garcia-Cazorla, A., Artuch, R., … Puelles, L. (2013). Development of the serotonergic cells in murine raphe nuclei and their relations with rhombomeric domains. *Brain Structure and Function*, *218*(5), 1229–1277. https://doi.org/10.1007/s00429-012-0456-8

Anadón, R., Molist, P., Rodríguez-Moldes, I., López, J. M., Quintela, I., Cerviño, M. C., … González, A. (2000). Distribution of choline acetyltransferase immunoreactivity in the brain of an elasmobranch, the lesser spotted dogfish (*Scyliorhinus canicula*). *Journal of Comparative Neurology*, *420*(2), 139–170. https://doi.org/10.1002/(SICI)1096-9861(20000501)420:2

Andrade, R., Huereca, D., Lyons, J. G., Andrade, E. M., & McGregor, K. M. (2015). 5-HT1A receptor-mediated autoinhibition and the control of serotonergic cell firing. *ACS Chemical Neuroscience*, *6*, 1110–1115. https://doi.org/10.1021/acschemneuro.5b00034

Backström, T., & Winberg, S. (2017). Serotonin coordinates responses to social stress—what we can learn from fish. *Frontiers in Neuroscience*, *11*, http://dx.doi.org/10.3389/fnins.2017.00595.

Bass, A. H. (1996). Shaping brain sexuality. *American Scientist*, *84*, 352–363.

Bass, A. H. (2008). Steroid-dependent plasticity of vocal motor systems: Novel insights from teleost fish. *Brain Research Reviews*, *57*(2), 299–308. https://doi.org/10.1016/j.brainresrev.2007.04.006

Bass, A. H., & Baker, R. (1990). Sexual dimorphisms in the vocal control system of a teleost fish: Morphology of physiologically identified neurons. *Journal of Neurobiology*, *21*(8), 1155–1168. https://doi.org/10.1002/neu.480210802

Bass, A. H., Bodnar, D. A., & Marchaterre, M. A. (2001). Acoustic nuclei in the medulla and midbrain of the vocalizing gulf toadfish (*Opsanus beta*). *Brain, Behavior and Evolution*, *57*(2), 63–79. https://doi.org/10.1159/000047226

Bass, A. H., Chagnaud, B. P., & Feng, N. Y. (2015). Comparative neurobiology of sound production in fishes. In F. Ladich (Ed.), *Sound communication in fishes* (Vol. 4, 1st ed., pp. 35–75). Vienna, Austria: Springer. https://doi.org/10.1007/978-3-7091-1846-7_2

Bass, A. H., Gilland, E. H., & Baker, R. (2008). Evolutionary origins for social vocalization in a vertebrate hindbrain–spinal compartment. *Science*, *321*(5887), 417–421. https://doi.org/10.1126/science.1157632

Bass, A. H., Horvath, B. J., & Brothers, E. B. (1996). Nonsequential developmental trajectories lead to dimorphic vocal circuitry for males with alternative reproductive tactics. *Journal of Neurobiology*, *30*(4), 493–504. https://doi.org/10.1002/(SICI)1097-4695(199608)30:4

Bass, A. H., & Marchaterre, M. A. (1989). Sound-generating (sonic) motor system in a teleost fish (*Porichthys notatus*): Sexual polymorphisms and general synaptology of sonic motor nucleus. *The Journal of Comparative Neurology*, *286*(2), 154–169. https://doi.org/10.1002/cne.902860203

Bass, A. H., Marchaterre, M. A., & Baker, R. (1994). Vocal-acoustic pathways in a teleost fish. *The Journal of Neuroscience*, *14*(7), 4025–4039.

Bass, A. H., Bodnar, D. A., & Marchaterre, M. A. (2000). Midbrain acoustic circuitry in a vocalizing fish. *The Journal of Comparative Neurology*, *419*(4), 505–531. http://dx.doi.org/10.1002/(sici)1096-9861(20000417)419:4<505::aid-cne7>3.0.co;2-3.

Bass, A. H., & McKibben, J. R. (2003). Neural mechanisms and behaviors for acoustic communication in teleost fish. *Progress in Neurobiology*, *69*(1), 1–26. https://doi.org/10.1016/S0301-0082(03)00004-2

Batten, T. F. C., Berry, P. A., Maqbool, A., Moons, L., & Vandesande, F. (1993). Immunolocalization of catecholamine enzymes, serotonin, dopamine and L-dopa in the brain of *Dicentrarchus labrax* (teleostei). *Brain Research Bulletin*, *31*(3–4), 233–252. https://doi.org/10.1016/0361-9230(93)90214-V

Berger, M., Gray, J. A., & Roth, B. L. (2009). The expanded biology of serotonin. *Annual Review of Medicine*, *60*(1), 355–366. https://doi.org/10.1146/annurev.med.60.042307.110802

Bolliet, V., & Ali, M. A. (1992). Immunohistochemical study of the development of serotoninergic neurons in the brain of the brook trout *Salvelinus fontinalis*. *Brain, Behavior and Evolution*, *40*(5), 234–249.

Bolliet, V., Perreault, S., & Ali, M. A. (1994). Development of serotonergic neurons in the brain of the mackerel, *Scomber scombrus*. An immunohistochemical study. *Journal of Fish Biology*, *44*(2), 241–253. https://doi.org/10.1111/j.1095-8649.1994.tb01202.x

Brantley, R. K., & Bass, A. H. (1988). Cholinergic neurons in the brain of a teleost fish (*Porichthys notatus*) located with a monoclonal antibody to choline acetyltransferase. *The Journal of Comparative Neurology*, *275*(1), 87–105. https://doi.org/10.1002/cne.902750108

Chagnaud, B. P., Baker, R., & Bass, A. H. (2011). Vocalization frequency and duration are coded in separate hindbrain nuclei. *Nature Communications*, *2*, 346. https://doi.org/10.1038/ncomms1349

Chagnaud, B. P., Zee, M. C., Baker, R., & Bass, A. H. (2012). Innovations in motoneuron synchrony drive rapid temporal modulations in vertebrate acoustic signaling. *Journal of Neurophysiology*, *107*(12), 3528–3542. https://doi.org/10.1152/jn.00030.2012

Cheng, C. W., Yan, C. H. M., Choy, S. W., Hui, M. N. Y., Hui, C.-C., & Cheng, S. H. (2007). Zebrafish homologue irx1a is required for the differentiation of serotonergic neurons. *Developmental Dynamics*, *236*(9), 2661–2667. https://doi.org/10.1002/dvdy.21272

Cohen, J. Y., Amoroso, M. W., & Uchida, N. (2015). Serotonergic neurons signal reward and punishment on multiple timescales. *eLife*, *4*, e06346. https://doi.org/10.7554/eLife.06346

Corio, M., Peute, J., & Steinbusch, H. W. (1991). Distribution of serotonin- and dopamine-immunoreactivity in the brain of the teleost *Clarias gariepinus*. *Journal of Chemical Neuroanatomy*, *4*(2), 79–95.

Dahlbom, S. J., Backström, T., Lundstedt-Enkel, K., & Winberg, S. (2012). Aggression and monoamines: Effects of sex and social rank in zebrafish (*Danio rerio*). *Behavioural Brain Research*, *228*(2), 333–338. https://doi.org/10.1016/j.bbr.2011.12.011

Dahlstroem, A., & Fuxe, K. (1964). Evidence for the existence of monoamine-containing neurons in the central nervous system. I. Demonstration of monoamines in the cell bodies of brain stem neurons. *Acta Physiologica Scandinavica. Supplementum*, *Suppl 232*, 1–55.

Deemyad, T., Metzen, M. G., Pan, Y., & Chacron, M. J. (2013). Serotonin selectively enhances perception and sensory neural responses to stimuli generated by same-sex conspecifics. *Proceedings of the National Academy of Sciences*, *110*(48), 19609–19614. https://doi.org/10.1073/pnas.1314008110

Dewan, A. K., & Tricas, T. C. (2014). Cytoarchitecture of the telencephalon in the coral reef multiband butterflyfish *Chaetodon multicinctus*-Perciformes. *Brain, Behavior and Evolution*, *84*(1), 31–50. https://doi.org/10.1159/000363124

Dufton, M., Hall, B. K., & Franz-Odendaal, T. A. (2012). Early lens ablation causes dramatic long-term effects on the shape of bones in the craniofacial skeleton of *Astyanax mexicanus*. *PLoS One*, *7*(11), e50308. https://doi.org/10.1371/journal.pone.0050308

Ekström, P. (1994). Developmental changes in the brain-stem serotonergic nuclei of teleost fish and neural plasticity. *Cellular and Molecular Neurobiology*, *14*(4), 381–393.

Ekström, P., & Ebbesson, S. O. (1989). Distribution of serotonin-immunoreactive neurons in the brain of sockeye salmon fry. *Journal of Chemical Neuroanatomy*, *2*(4), 201–213.

Ekström, P., Östholm, T., & Ebbesson, S. O. E. (1992). A morphometric study of age-related changes in serotonin-immunoreactive cell groups in the brain of the coho salmon, *Oncorhynchus kisutch* walbaum. *Experimental Neurology*, *116*(2), 204–209. https://doi.org/10.1016/0014-4886(92)90169-Q

Ekström, P., & Van Veen, T. (1984). Distribution of 5-hydroxytryptamine (serotonin) in the brain of the teleost *Gasterosteus aculeatus* L. *The Journal of Comparative Neurology*, *226*(3), 307–320. https://doi.org/10.1002/cne.902260302

Feng, N., & Bass, A. (2017). Neural, hormonal, and genetic mechanisms of alternative reproductive tactics: Vocal fish as model systems (pp. 47–68). Part of Hormones, brain, and behavior, ISBN 9780128035924. https://doi.org/10.1016/B978-0-12-803592-4.00018-3

Fine, M. L., & Perini, M. A. (1994). Sound production evoked by electrical stimulation of the forebrain in the oyster toadfish. *Journal of Comparative Physiology. A, Sensory, Neural, and Behavioral Physiology*, *174*(2), 173–185.

Fink, K. B., & Göthert, M. (2007). 5-HT receptor regulation of neurotransmitter release. *Pharmacological Reviews*, *59*(4), 360–417. https://doi.org/10.1124/pr.107.07103

Forlano, P. M., & Bass, A. H. (2011). Neural and hormonal mechanisms of reproductive-related arousal in fishes. *Hormones and Behavior*, *59*(5), 616–629. https://doi.org/10.1016/j.yhbeh.2010.10.006

Forlano, P. M., Deitcher, D. L., Myers, D. A., & Bass, A. H. (2001). Anatomical distribution and cellular basis for high levels of aromatase activity in the brain of teleost fish: Aromatase enzyme and mRNA expression identify glia as source. *The Journal of Neuroscience*, *21*(22), 8943–8955.

Forlano, P. M., Ghahramani, Z. N., Monestime, C. M., Kurochkin, P., Chernenko, A., & Milkis, D. (2015). Catecholaminergic innervation of central and peripheral auditory circuitry varies with reproductive state in female midshipman fish, *Porichthys notatus*. *PLoS One*, *10*(4), e0121914. https://doi.org/10.1371/journal.pone.0121914

Forlano, P. M., Kim, S. D., Krzyminska, Z. M., & Sisneros, J. A. (2014). Catecholaminergic connectivity to the inner ear, central auditory, and vocal motor circuitry in the plainfin midshipman fish *Porichthys notatus*. *Journal of Comparative Neurology*, *522*(13), Spc1. https://doi.org/10.1002/cne.23638

Forlano, P. M., Maruska, K. P., Sisneros, J. A., & Bass, A. H. (2016). Hormone-dependent plasticity of auditory systems in fishes. In A. Bass, J. Sisneros, A. Popper, & R. Fay (Eds.), *Hearing and hormones*, Springer handbook of auditory research, Vol. 57, (15–51). Cham, Switzerland: Springer.

Forlano, P. M., Sisneros, J. A., Rohmann, K. N., & Bass, A. H. (2015). Neuroendocrine control of seasonal plasticity in the auditory and vocal systems of fish. *Frontiers in Neuroendocrinology*, *37*, 129–145. https://doi.org/10.1016/j.yfrne.2014.08.002

Gabriel, J. P., Mahmood, R., Kyriakatos, A., Söll, I., Hauptmann, G., Calabrese, R. L., & El Manira, A. (2009). Serotonergic modulation of locomotion in zebrafish—Endogenous release and synaptic mechanisms. *The Journal of Neuroscience*, *29*(33), 10387–10395.

Gaspar, P., & Lillesaar, C. (2012). Probing the diversity of serotonin neurons. *Philosophical Transactions of the Royal Society B: Biological Sciences*, *367*(1601), 2382–2394. https://doi.org/10.1098/rstb.2011.0378

Ghahramani, Z. N., Timothy, M., Kaur, G., Gorbonosov, M., Chernenko, A., & Forlano, P. M. (2015). Catecholaminergic fiber innervation of the vocal motor system is intrasexually dimorphic in a teleost with alternative reproductive tactics. *Brain, Behavior and Evolution*, *86*(2), 131–144. https://doi.org/10.1159/000438720

Gilland, E., Straka, H., Wong, T. w., Baker, R., & Zottoli, S. j. (2014). A hindbrain segmental scaffold specifying neuronal location in the adult goldfish, *Carassius auratus*. *Journal of Comparative Neurology*, *522*(10), 2446–2464. https://doi.org/10.1002/cne.23544

Goebrecht, G. K. E., Kowtoniuk, R. A., Kelly, B. G., & Kittelberger, J. M. (2014). Sexually-dimorphic expression of tyrosine hydroxylase immunoreactivity in the brain of a vocal teleost fish (*Porichthys notatus*). *Journal of Chemical Neuroanatomy*, *56*(Suppl C), 13–34. https://doi.org/10.1016/j.jchemneu.2014.01.001

Goodson, J. L., & Bass, A. H. (2002). Vocal-acoustic circuitry and descending vocal pathways in teleost fish: Convergence with terrestrial vertebrates reveals conserved traits. *The Journal of Comparative Neurology*, *448*(3), 298–322. https://doi.org/10.1002/cne.10258

Goodson, J. L., Evans, A. K., & Bass, A. H. (2003). Putative isotocin distributions in sonic fish: Relation to vasotocin and vocal-acoustic circuitry. *The Journal of Comparative Neurology*, *462*(1), 1–14. https://doi.org/10.1002/cne.10679

Gotow, T., Triller, A., & Korn, H. (1990). Differential distribution of serotoninergic inputs on the goldfish mauthner cell. *The Journal of Comparative Neurology*, *292*(2), 255–268. http://dx.doi.org/10.1002/cne.902920208.

Hanks, J. B., & González-Maeso, J. (2013). Animal models of serotonergic psychedelics. *ACS Chemical Neuroscience*, *4*(1), 33–42. https://doi.org/10.1021/cn300138m

Hermann, D. M., Luppi, P.-H., Peyron, C., Hinckel, P., & Jouvet, M. (1997). Afferent projections to the rat nuclei raphe magnus, raphe pallidus and reticularis gigantocellularis pars α demonstrated by iontophoretic application of choleratoxin (subunit b). *Journal of Chemical Neuroanatomy*, *13*(1), 1–21. http://dx.doi.org/10.1016/s0891-0618(97)00019-7.

Hornung, J.-P. (2003). The human raphe nuclei and the serotonergic system. *Journal of Chemical Neuroanatomy*, *26*(4), 331–343. http://dx.doi.org/10.1016/j.jchemneu.2003.10.002.

Hurley, L. M., & Pollak, G. D. (2005). Serotonin modulates responses to species-specific vocalizations in the inferior colliculus. *Journal of Comparative Physiology. A, Neuroethology, Sensory, Neural, and Behavioral Physiology*, *191*(6), 535–546. https://doi.org/10.1007/s00359-005-0623-y

Hurley, L. M., & Sullivan, M. R. (2012). From behavioral context to receptors: Serotonergic modulatory pathways in the IC. *Frontiers in Neural Circuits*, *6*, 58. https://doi.org/10.3389/fncir.2012.00058

Jacobs, B. L., & Fornal, C. A. (1993). 5-HT and motor control: A hypothesis. *Trends in Neurosciences*, *16*(9), 346–352.

Jacobs, B. L., & Fornal, C. A. (2010). Chapter 2.1–Activity of brain serotonergic neurons in relation to physiology and behavior. In C. P. Müller & B. L. Jacobs (Eds.), *Handbook of the Behavioral Neurobiology of Serotonin*, Handbook of behavioral neuroscience, (Vol. 21, pp. 153–162). London, UK: Elsevier. https://doi.org/10.1016/S1569-7339(10)70076-X

JASP Team. (2019). JASP (version 0.11.1) [computer software]. Retrieved from https://jasp-stats.org/

Jordan, P. M., Fettis, M., & Holt, J. C. (2015). Efferent innervation of turtle semicircular canal cristae: Comparisons with bird and mouse. *Journal of Comparative Neurology*, *523*(8), 1258–1280. https://doi.org/10.1002/cne.23738

Kah, O., & Chambolle, P. (1983). Serotonin in the brain of the goldfish, *Carassius auratus*. An immunocytochemical study. *Cell and Tissue Research*, *234*(2), 319–333.

Kaslin, J., & Panula, P. (2001). Comparative anatomy of the histaminergic and other aminergic systems in zebrafish (*Danio rerio*). *The Journal of Comparative Neurology*, *440*(4), 342–377.

Khan, I. A., & Thomas, P. (1993). Immunocytochemical localization of serotonin and gonadotropin-releasing hormone in the brain and pituitary gland of the Atlantic croaker *Micropogonias undulatus*. *General and Comparative Endocrinology*, *91*(2), 167–180. https://doi.org/10.1006/gcen.1993.1116

Kittelberger, J. M., & Bass, A. H. (2012). Vocal-motor and auditory connectivity of the midbrain periaqueductal gray in a teleost fish. *The Journal of Comparative Neurology*, *521*, 791–812. https://doi.org/10.1002/cne.23202

Kittelberger, J. M., Land, B. R., & Bass, A. H. (2006). Midbrain periaqueductal gray and vocal patterning in a teleost fish. *Journal of Neurophysiology*, *96*(1), 71–85. https://doi.org/10.1152/jn.00067.2006

Kiyasova, V., & Gaspar, P. (2011). Development of raphe serotonin neurons from specification to guidance. *European Journal of Neuroscience*, *34*(10), 1553–1562. https://doi.org/10.1111/j.1460-9568.2011.07910.x

Kuscha, V., Barreiro-Iglesias, A., Becker, C. G., & Becker, T. (2011). Plasticity of tyrosine hydroxylase and serotonergic systems in the regenerating spinal cord of adult zebrafish. *The Journal of Comparative Neurology.*, *520*, 933–951. https://doi.org/10.1002/cne.22739

Li, Y.-Q., Takada, M., & Mizuno, N. (1993). The sites of origin of serotoninergic afferent fibers in the trigeminal motor, facial, and hypoglossal nuclei in the rat. *Neuroscience Research*, *17*(4), 307–313. https://doi.org/10.1016/0168-0102(93)90114-6

Lillesaar, C. (2011). The serotonergic system in fish. *Journal of Chemical Neuroanatomy*, *41*(4), 294–308. https://doi.org/10.1016/j.jchemneu.2011.05.009

Lillesaar, C., Stigloher, C., Tannhäuser, B., Wullimann, M. F., & Bally-Cuif, L. (2009). Axonal projections originating from raphe serotonergic neurons in the developing and adult zebrafish, *Danio rerio*, using transgenics to visualize raphe-specific pet1 expression. *The Journal of Comparative Neurology*, *512*(2), 158–182. https://doi.org/10.1002/cne.21887

Lillesaar, C., Tannhäuser, B., Stigloher, C., Kremmer, E., & Bally-Cuif, L. (2007). The serotonergic phenotype is acquired by converging genetic mechanisms within the zebrafish central nervous system.

Developmental Dynamics, *236*(4), 1072–1084. https://doi.org/10.1002/dvdy.21095

López, J. M., Perlado, J., Morona, R., Northcutt, R. G., & González, A. (2013). Neuroanatomical organization of the cholinergic system in the central nervous system of a basal actinopterygian fish, the Senegal bichir *Polypterus senegalus*. *Journal of Comparative Neurology*, *521*(1), 24–49. https://doi.org/10.1002/cne.23155

Lorenzi, V., & Grober, M. S. (2012). Immunohistochemical localization of serotonin in the brain during natural sex change in the hermaphroditic goby *Lythrypnus dalli*. *General & Comparative Endocrinology*, *175*(3), 527–536. https://doi.org/10.1016/j.ygcen.2011.12.018

Lu, Z., & Fay, R. R. (1995). Acoustic response properties of single neurons in the central posterior nucleus of the thalamus of the goldfish, *Carassius auratus*. *Journal of Comparative Physiology A*, *176*(6), 747–760. https://doi.org/10.1007/BF00192623

Mager, E. M., Medeiros, L. R., Lange, A. P., & McDonald, M. D. (2012). The toadfish serotonin 5-HT2A receptor: Molecular characterization and its potential role in urea excretion. *Comparative Biochemistry and Physiology Part A: Molecular & Integrative Physiology*, *163*, 319–326.

Marín, O., Smeets, W. J. A. J., & González, A. (1997). Distribution of choline acetyltransferase immunoreactivity in the brain of anuran (*Rana perezi*, *Xenopus laevis*) and urodele (*Pleurodeles waltl*) amphibians. *The Journal of Comparative Neurology*, *382*(4), 499–534.

Maximino, C., & Herculano, A. M. (2010). A review of monoaminergic neuropsychopharmacology in zebrafish. *Zebrafish*, *7*(4), 359–378. https://doi.org/10.1089/zeb.2010.0669

May, P. J., Baker, H., Vidal, P.-P., Spencer, R. F., & Baker, R. (1987). Morphology and distribution of serotoninergic and oculomotor internuclear neurons in the cat midbrain. *Journal of Comparative Neurology*, *266*(2), 150–170.

McIver, E. L., Marchaterre, M. A., Rice, A. N., & Bass, A. H. (2014). Novel underwater soundscape: Acoustic repertoire of plainfin midshipman fish. *Journal of Experimental Biology*, *217*(13), 2377–2389. https://doi.org/10.1242/jeb.102772

McLean, D. L., & Fetcho, J. R. (2004). Ontogeny and innervation patterns of dopaminergic, noradrenergic, and serotonergic neurons in larval zebrafish. *The Journal of Comparative Neurology*, *480*(1), 38–56. https://doi.org/10.1002/cne.20280

Medeiros, L. R., Mager, E. M., Grosell, M., & McDonald, M. D. (2010). The serotonin subtype 1A receptor regulates cortisol secretion in the Gulf toadfish, *Opsanus beta*. *General and Comparative Endocrinology*, *168*(3), 377–387. https://doi.org/10.1016/j.ygcen.2010.05.004

Medina, L., & Reiner, A. (1994). Distribution of choline acetyltransferase immunoreactivity in the pigeon brain. *Journal of Comparative Neurology*, *342*(4), 497–537. https://doi.org/10.1002/cne.903420403

Meek, J., & Joosten, H. W. J. (1989). Distribution of serotonin in the brain of the mormyrid teleost *Gnathonemus petersii*. *Journal of Comparative Neurology*, *281*(2), 206–224. https://doi.org/10.1002/cne.902810205

Mennigen, J. A., Stroud, P., Zamora, J. M., Moon, T. W., & Trudeau, V. L. (2011). Pharmaceuticals as neuroendocrine disruptors: Lessons learned from fish on Prozac. *Journal of Toxicology & Environmental Health: Part B*, *14*(5–7), 387–412. https://doi.org/10.1080/10937404.2011.578559

Miles, G. B., & Sillar, K. T. (2011). Neuromodulation of vertebrate locomotor control networks. *Physiology*, *26*(6), 393–411. https://doi.org/10.1152/physiol.00013.2011

Mohr, R. A., Chang, Y., Bhandiwad, A. A., Forlano, P. M., & Sisneros, J. A. (2018). Brain activation patterns in response to conspecific and heterospecific social acoustic signals in female plainfin midshipman fish, porichthys notatus. *Brain, Behavior and Evolution*, *91*(1), 31–44. http://dx.doi.org/10.1159/000487122.

Mueller, T., Vernier, P., & Wullimann, M. F. (2004). The adult central nervous cholinergic system of a neurogenetic model animal, the zebrafish *Danio rerio*. *Brain Research*, *1011*(2), 156–169. https://doi.org/10.1016/j.brainres.2004.02.073

Neelkantan, N., Mikhaylova, A., Stewart, A. M., Arnold, R., Gjeloshi, V., Kondaveeti, D., … Kalueff, A. V. (2013). Perspectives on zebrafish models of hallucinogenic drugs and related psychotropic compounds. *ACS Chemical Neuroscience*, *4*(8), 1137–1150. https://doi.org/10.1021/cn400090q

Nieuwenhuys, R. (2011). The structural, functional, and molecular organization of the brainstem. *Frontiers in Neuroanatomy*, *5*, 33. https://doi.org/10.3389/fnana.2011.00033

Oliveri, D., Candiani, S., Parodi, M., Bertini, E., & Pestarino, M. (2005). A serotonergic system in the brain of the Antarctic fish, *Trematomus bernacchii*. *Polar Biology*, *28*(5), 366–371. https://doi.org/10.1007/s00300-004-0706-1

Olsson, C. (2011). Calbindin immunoreactivity in the enteric nervous system of larval and adult zebrafish (*Danio rerio*). *Cell and Tissue Research*, *344*(1), 31–40. https://doi.org/10.1007/s00441-011-1135-4

Parent, M., Wallman, M. J., Gagnon, D., & Parent, A. (2011). Serotonin innervation of basal ganglia in monkeys and humans. *Journal of Chemical Neuroanatomy*, *41*, 256–265.

Perelmuter, J. T., & Forlano, P. M. (2017). Connectivity and ultrastructure of dopaminergic innervation of the inner ear and auditory efferent system of a vocal fish. *Journal of Comparative Neurology*, *525*(9), 2090–2108. https://doi.org/10.1002/cne.24177

Pérez, S. E., Yáñez, J., Marín, O., Anadón, R., González, A., & Rodríguez-Moldes, I. (2000). Distribution of choline acetyltransferase (ChAT) immunoreactivity in the brain of the adult trout and tract-tracing observations on the connections of the nuclei of the isthmus. *The Journal of Comparative Neurology*, *428*(3), 450–474. https://doi.org/10.1002/1096-9861(20001218)428:3

Petersen, C. L., & Hurley, L. M. (2017). Putting it in context: Linking auditory processing with social behavior circuits in the vertebrate brain. *Integrative and Comparative Biology*, *57*, 865–877. https://doi.org/10.1093/icb/icx055

Petersen, C. L., Timothy, M., Kim, D. S., Bhandiwad, A. A., Mohr, R. A., Sisneros, J. A., & Forlano, P. M. (2013). Exposure to advertisement calls of reproductive competitors activates vocal-acoustic and catecholaminergic neurons in the plainfin midshipman fish, *Porichthys notatus*. *PLoS One*, *8*(8), e70474. https://doi.org/10.1371/journal.pone.0070474

Pollak Dorocic, I., Fürth, D., Xuan, Y., Johansson, Y., Pozzi, L., Silberberg, G., … Meletis, K. (2014). A whole-brain atlas of inputs to serotonergic neurons of the dorsal and median raphe nuclei. *Neuron*, *83*(3), 663–678. https://doi.org/10.1016/j.neuron.2014.07.002

Pombal, M. A., Marín, O., & González, A. (2001). Distribution of choline acetyltransferase-immunoreactive structures in the lamprey brain. *Journal of Comparative Neurology*, *431*(1), 105–126. https://doi.org/10.1002/1096-9861(20010226)431:1

Remage-Healey, L., & Bass, A. H. (2004). Rapid, Hierarchical Modulation of Vocal Patterning by Steroid Hormones. *Journal of Neuroscience*, *24*(26), 5892–5900. http://dx.doi.org/10.1523/jneurosci.1220-04.2004.

Reyes, C., Fong, A. Y., Brink, D. L., & Milsom, W. K. (2014). Distribution and innervation of putative arterial chemoreceptors in the bullfrog (*Rana catesbeiana*). *Journal of Comparative Neurology*, *522*(16), 3754–3774. https://doi.org/10.1002/cne.23640

Rhodes, H. J., Yu, H. J., & Yamaguchi, A. (2007). Xenopus vocalizations are controlled by a sexually differentiated hindbrain central pattern generator. *The Journal of Neuroscience*, *27*(6), 1485–1497. https://doi.org/10.1523/JNEUROSCI.4720-06.2007

Rink, E., & Wullimann, M. F. (2001). The teleostean (zebrafish) dopaminergic system ascending to the subpallium (striatum) is located in the basal diencephalon (posterior tuberculum). *Brain Research*, *889*(1–2), 316–330. https://doi.org/10.1016/S0006-8993(00)03174-7

Rodríguez-Gómez, F. J., Rendón-Unceta, M. C., Sarasquete, C., & Muñoz-Cueto, J. A. (2000). Distribution of serotonin in the brain of the

Senegalese sole, *Solea senegalensis*: An immunohistochemical study. *Journal of Chemical Neuroanatomy*, *18*(3), 103–115.

Rodríguez-Moldes, I., Molist, P., Adrio, F., Pombal, M. A., Yáñez, S. E. P., Mandado, M., … Anadón, R. (2002). Organization of cholinergic systems in the brain of different fish groups: A comparative analysis. *Brain Research Bulletin*, *57*(3), 331–334. https://doi.org/10.1016/S0361-9230(01)00700-6

Rosner, E., Rohmann, K. N., Bass, A. H., & Chagnaud, B. P. (2018). Inhibitory and modulatory inputs to the vocal central pattern generator of a teleost fish. *Journal of Comparative Neurology*, *526*, 1368–1388. https://doi.org/10.1002/cne.24411

Schindelin, J., Rueden, C. T., Hiner, M. C., & Eliceiri, K. W. (2015). The ImageJ ecosystem: An open platform for biomedical image analysis. *Molecular Reproduction and Development*, *82*(7–8), 518–529. doi.org/10.1002/mrd.22489

Sisneros, J. A., Forlano, P. M., Knapp, R., & Bass, A. H. (2004). Seasonal variation of steroid hormone levels in an intertidal-nesting fish, the vocal plainfin midshipman. *General and Comparative Endocrinology*, *136*(1), 101–116. https://doi.org/10.1016/j.ygcen.2003.12.007

Smeets, W. J. A. J., & González, A. (2000). Catecholamine systems in the brain of vertebrates: New perspectives through a comparative approach. *Brain Research Reviews*, *33*(2), 308–379. https://doi.org/10.1016/S0165-0173(00)00034-5

Tay, T. L., Ronneberger, O., Ryu, S., Nitschke, R., & Driever, W. (2011). Comprehensive catecholaminergic projectome analysis reveals single-neuron integration of zebrafish ascending and descending dopaminergic systems. *Nature Communications*, *2*, 171. https://doi.org/10.1038/ncomms1171

Telgkamp, P., Combs, N., & Smith, G. T. (2007). Serotonin in a diencephalic nucleus controlling communication in an electric fish: Sexual dimorphism and relationship to indicators of dominance. *Developmental Neurobiology*, *67*(3), 339–354. https://doi.org/10.1002/dneu.20356

Timothy, M., & Forlano, P. M. (2019). A versatile macro-based neurohistological image analysis suite for ImageJ focused on automated and standardized user interaction and reproducible data output. *Journal of Neuroscience Methods*, *324*, 108286. https://doi.org/10.1016/j.jneumeth.2019.04.009

Timothy, M., Ghahramani, Z. N., Gorbonosov, M., Ferrari, M., & Forlano, P. M. (2014). Serotonergic differences in vocal motor circuitry and the caudal raphe of male midshipman fish morphotypes. Paper presented at the Annual Meeting of the Society for Neuroscience, Washington, D.C.

Vertes, R. P., & Crane, A. M. (1997). Distribution, quantification, and morphological characteristics of serotonin-immunoreactive cells of the supralemniscal nucleus (B9) and pontomesencephalic reticular formation in the rat. *The Journal of Comparative Neurology*, *378*(3), 411–424. https://doi.org/10.1002/(SICI)1096-9861(19970217)378:3

Vertes, R. P., & Linley, S. B. (2008). Efferent and afferent connections of the dorsal and median raphe nuclei in the rat. In J. M. Monti, S. R. Pandi-Perumal, B. L. Jacobs, & D. J. Nutt (Eds.), *Serotonin and sleep: Molecular, functional and clinical aspects* (pp. 69–102). Basel, Switzerland: Birkhäuser.

Weeg, M. S. (2005). Vocal pathways modulate efferent neurons to the inner ear and lateral line. *Journal of Neuroscience*, *25*(25), 5967–5974. https://doi.org/10.1523/JNEUROSCI.0019-05.2005

Weeg, M. S., & Bass, A. H. (2000). Central lateral line pathways in a vocalizing fish. *The Journal of Comparative Neurology*, *418*(1), 41–64.

Whitaker, K. W., Neumeister, H., Huffman, L. S., Kidd, C. E., Preuss, T., & Hofmann, H. A. (2011). Serotonergic modulation of startle-escape plasticity in an African cichlid fish: A single-cell molecular and physiological analysis of a vital neural circuit. *Journal of Neurophysiology*, *106*(1), 127–137. https://doi.org/10.1152/jn.01126.2010

Wibowo, E., Brockhausen, J., & Köppl, C. (2009). Efferent innervation to the auditory basilar papilla of scincid lizards. *The Journal of Comparative Neurology*, *516*(1), 74–85. https://doi.org/10.1002/cne.22101

Wood, W. E., Lovell, P. V., Mello, C. V., & Perkel, D. J. (2011). Serotonin, via HTR2 receptors, excites neurons in a cortical-like premotor nucleus necessary for song learning and production. *The Journal of Neuroscience*, *31*(39), 13808–13815. https://doi.org/10.1523/JNEUROSCI.2281-11.2011

Xavier, A. L., Fontaine, R., Bloch, S., Affaticati, P., Jenett, A., Demarque, M., … Yamamoto, K. (2017). Comparative analysis of monoaminergic cerebrospinal fluid-contacting cells in Osteichthyes (bony vertebrates). *Journal of Comparative Neurology*, *525*, 2265–2283. https://doi.org/10.1002/cne.24204

Yin, J.-B., Wu, H.-H., Dong, Y.-L., Zhang, T., Wang, J., Zhang, Y., … Li, Y.-Q. (2014). Neurochemical properties of BDNF-containing neurons projecting to rostral ventromedial medulla in the ventrolateral periaqueductal gray. *Frontiers in Neural Circuits*, *8*, 137. https://doi.org/10.3389/fncir.2014.00137

Yu, H. J., & Yamaguchi, A. (2009). 5-HT2C-like receptors in the brain of *Xenopus laevis* initiate sex-typical fictive vocalizations. *Journal of Neurophysiology*, *102*(2), 752–765. https://doi.org/10.1152/jn.90469.2008

Yu, H. J., & Yamaguchi, A. (2010). Endogenous serotonin acts on 5-HT2C-like receptors in key vocal areas of the brain stem to initiate vocalizations in *Xenopus laevis*. *Journal of Neurophysiology*, *103*(2), 648–658. https://doi.org/10.1152/jn.00827.2009

How to cite this article: Timothy M, Forlano PM. Serotonin distribution in the brain of the plainfin midshipman: Substrates for vocal-acoustic modulation and a reevaluation of the serotonergic system in teleost fishes. *J Comp Neurol*. 2020; 528:3451–3478. https://doi.org/10.1002/cne.24938